Palmer LTER: Patterns of Distribution of Five Dominant Zooplankton Species in the Epipelagic Zone West of the Antarctic Peninsula, 1993 - 2004

Robin M. Ross[1], Langdon B. Quetin[1], Douglas G. Martinson[2], Rich Iannuzzi[2], Sharon Stammerjohn[3], and Ray C. Smith[3]

[1]Marine Science Institute, University of California at Santa Barbara, Santa Barbara, CA 93106-6150

[2]Lamont Doherty Earth Observatory, Columbia University, Palisades, NY

[3]NASA Goddard Institute for Space Studies, New York, NY 10025

[4]Institute for Computational Earth System Science, University of California at Santa Barbara, Santa Barbara, CA 93106

ABSTRACT

Variability in the temporal-spatial distribution and abundance of zooplankton was documented each summer on the Palmer Long-Term Ecological Research (LTER) grid west of the Antarctic Peninsula between Anvers and Adelaide Islands during a 12-yr time-series. Oblique tows to 120 m with a 2 x 2 m fixed-frame net were made at about 50 stations per year in the January/February time period between 1993 and 2004. The numerically dominant macro- and mesozooplanktonic species > 2 mm included 3 species of euphausiids (*Euphausia superba,* Antarctic krill*; Thysanoëssa macrura*; *Euphausia crystallorophias*, ice krill), a shelled pteropod (*Limacina helicina*), and a salp (*Salpa thompsoni*). Life cyles, life spans, and habitat varied among these species. Abundance data from each year were allocated to 100 km by 20 km (alongshore by on/offshore) grid cells centered on cardinal transect lines and stations within the Palmer LTER grid. The long-term mean or climatology and means for each year were used to calculate annual anomalies across the grid. Principal Components Analysis (PCA) was used to analyze for patterns and trends in the spatial/temporal variability of the 5 species. Questions included whether there are groups of species with similar patterns, and whether population cycles, species interactions or seasonal sea-ice parameters were correlated with the detected patterns. Patterns in the climatology were distinct, and matched those of physical parameters. Common features included higher abundance in the north than the south, independent of the cross-shelf gradients, and cross-shelf gradients with highs in abundance either inshore (*E. crystallorophias*) or offshore (*S. thompsoni*). Anomalies revealed either cycles in the population, as episodic recruitment in Antarctic krill, or changes in anomaly pattern between the first and second half of the sampling period. The 1998 year, which coincided with a rapid change from negative to positive phase in the SOI, emerged as a year of significant anomalies for several species,

and marked a change in anomaly patterns for others. PCA analysis showed that the pattern of cumulative variance with increasing number of modes was distinctly different for the shorter-lived versus the longer-lived species, as the first mode accounted for nearly 50% of the variance accounted for the shorter-lived species and less than 25% for the longer-lived species. This suggested that the mechanisms driving variability in the temporal/spatial distribution of the shorter-lived, more oceanic species were less complex and more direct than those for the longer-lived euphausiids. Evidence from both the anomaly plots and the trend analysis suggested that salps have been more consistently present across the shelf from 1999 to present, and that the range of *L. helicina* has been expanding. With shorter life spans, these two species can respond more quickly to the increasing heat content on the shelf in this region. The cross-correlation analysis illustrated the negative correlation between salps and ice advance and the number of ice days, and the positive correlation between the presence of ice krill and the day of ice retreat. These results suggest that several environmental controls on distribution and abundance of these species were linked to seasonal sea-ice dynamics.

1. Introduction

Zooplankton assemblages in the Southern Ocean have been broadly associated with different water masses with different sea-ice influences from the time of the Discovery Expeditions (Mackintosh, 1936) – warm-water species within the northern 'oceanic' zone, colder-water species within a zone influenced by seasonal pack ice, and species closely associated with a cold continental shelf zone close to the continent which characteristically contains permanent summer ice. Recently, Ward et al. (2004), in a recent large-scale investigation of the zooplankton community structure in relation to frontal zones in the southwest Atlantic, found that the relative numbers of copepods, euphausiids and salps varied with the distribution of ice-influenced water. In relatively ice-free and deeper oceanic waters, copepods were orders of magnitude more abundant than in colder waters influenced by sea-ice, particularly south of the Southern Boundary of the Antarctic Circumpolar Current (SBACC). The abundance of both salps and Antarctic krill (*Euphausia superba*) doubled south of the Southern Antarctic Circumpolar Current Front (SACCF) (Ward et al., 2004). In waters closer to the Peninsula where schools of krill occur, the biomass of Antarctic krill is often higher than that of the copepods (Hopkins and Lancraft, 1985; Brinton and Antezana, 1984; Lancraft et al., 2004). Other taxonomic groups (worms, chaetognaths and pteropods) usually contribute only a small percent (<10%) to the zooplankton biomass in the Antarctic Peninsula region (Schnack-Schiel and Mujica, 1994).

The Palmer Long-Term Ecological Research (LTER) program was established in 1990, and its summer regional time-series began in January 1993. The Palmer LTER is a multi-disciplinary program focused on the structure and function of the pelagic marine ecosystem west of the Antarctic Peninsula. At its inception, the overarching hypothesis was that structure and function of all levels of the food web were controlled by physical

factors, primarily seasonal sea-ice dynamics. The study region lies mid-way down the relatively broad shelf on the western side of the Antarctic Peninsula (WAP) encompassing the slope, shelf break and relatively deep continental shelf, and belongs to the coastal and continental shelf zone (CCSZ) and seasonal sea-ice zone (SIZ), as defined by Treguer and Jacques (1992). The Antarctic Circumpolar Current (ACC) may influence distributions as the SBACC is found close to the slope in this region (Orsi et al., 1995), and upper circum-polar deep-water (UCDW) floods the shelf (Martinson et al., this volume). Within the region, there is also considerable variation in the depth of the water column, the productivity and community composition of the phytoplankton community, and such aspects of seasonal sea-ice dynamics as summer ice extent. Larger scale or longer-term effects, such as large-scale movements of water masses due to atmospheric shifts (Priddle et al., 1988), climate cycles such as ENSO (Quetin et al., 1996; Quetin and Ross, 2003) or regime shifts and the rapidly changing climate in this region of the Antarctic (Domack et al., 2003; Vaughan et al., 2003; Ducklow et al., 2007) may lead to variability in the zooplankton community at different time scales. The abundance and distribution of the zooplankton community in the epipelagic zone of the Palmer LTER study region was an integral component of the overall program. The macrozooplanktonic species, particularly Antarctic krill and other species > 2 cm, form the primary link between the primary producers and consumers such as seabirds and seals in the Southern Ocean. With the inclusion of the larger mesozooplankton (2 – 20 mm) this community of larger zooplankton may also impact the abundance and composition of the phytoplankton community through the effects of grazing activity. Within the Palmer LTER study region, numerically dominant species of macrozooplankton and larger mesozooplankton within the epipelagic zone include several species of euphausiids (*Euphausia superba*, *Thysanöessa macrura*, and *E.*

crystallorophias), a herbivorous shelled pteropod (*Limacina helicina*) and a salp *(Salpa thompsoni*). In waters deeper than 2000 m we would expect to find *S. thompsonni*, which have been postulated to be a potential competitor for Antarctic krill (Loeb et al., 1997). In shelf break and shelf regions we expect to find two species of euphausiids, Antarctic krill (*E. superba*) and *Thysanöessa macrura*, and *Limacina helicina*. However, species typical of oceanic water masses such as *S. thompsoni* may occur over much of the shelf region in varying mixes with the more restricted occupants. In areas of the Palmer LTER study region *E. crystallorophias* is generally restricted to the permanent pack ice zone or cold continental shelf water as is found at higher latitudes (Smith and Schnack-Schiel, 1990).

The life cycles and life spans of the 5 species differ. *Salpa thompsoni* has the shortest life span and a complex life cycle, alternating sexual and asexual (budding) generations within a single year. On a broad scale, budding of chains of aggregates begins in austral spring, and sexual reproduction occurs at the end of a salp bloom (Foxton, 1966). Under favorable conditions, *S. thompsoni* can reproduce rapidly, forming swarms in which the aggregate form dominates. Environmental conditions favoring salp blooms are not well understood, although low chlorophyll concentrations and the presence of small phytoplankton cells are thought to be factors (Harbison et al., 1986; Kawaguchi et al., 1999; Perissinotto and Pakhomov, 1998). The timing of *S. thompsoni* blooms during the summer appears to be correlated with latitude, with blooms earlier in the northern waters west of the Antarctic Peninsula than the south (Ross et al., 1996). Less is known about *Limacina helicina*. Spawning appears to start in January, and the largest specimens are found in the summer (Dec – Feb) (Lalli and Gilmer, 1989). In the Arctic, the life span of the same species is thought to be 1.5 to 2 yr (Lalli and Gilmer, 1989). All three euphausiids are broadcast spawners (Ross and Quetin, 2000). Life spans and spawning

times were summarized in Ross et al. (1996). *Thysanöessa macrura* spawns the earliest (September) and has the shortest life span (4 yr). *Euphausia crystallorophias* spawns in early November, and lives 4 (males) to 5 (females) yr. *E. superba*, the largest and longest lived (6-7 yr) euphausiid, spawns in summer (Dec – Mar), with timing dependent on latitude and feeding conditions.

The objectives of this study are to: (1) document patterns of distribution and abundance in time and space of 5 dominant macro- and mesozooplanktonic species ≥ 2 mm in the Palmer LTER region, (2) investigate whether there are groups of species with similar patterns, and (3) explore whether population cycles, species interactions or environmental variables correlate with these patterns. Specifically we used Principal Components Analysis (PCA) to investigate patterns and possible trends in the spatial/temporal variability between 1993 and 2004 of the above 5 species. The choice of PCA was based on our desire to establish a common template for analysis and comparison of temporal/spatial variability among the various data sets collected by the Palmer LTER in order to facilitate testing of hypotheses with the long-term data sets. The approach is consistent with other oceanographic disciplines, e.g., physics and climatology, which typically decompose space-time fields in this manner. Similar analyses have yielded considerable insights into the study of climate, where it is now clear that the major components of our climate system are consistently contained in physically-meaningful modes that can be captured statistically. As the first step in understanding interactions, we also present comparisons of the long-term mean distribution of the 5 species among themselves and among each species and seasonal sea-ice parameters representing timing of advance and retreat, duration of ice extent (number of days between advance and retreat), and persistence of ice cover (percent of time cell covered with sea-ice between advance and retreat) (Stammerjohn et al., this

volume). This manuscript establishes the basic distribution patterns of dominant macro- and mesozooplankton species, and the results will serve as the basis of future explorations of physical/biological interactions.

2. Materials and Methods

2.1 Study area, cruise times and stations occupied

The Palmer LTER grid consists of transect lines spaced 100 km apart alongshore and stations spaced 20 km apart from the coast to 200 km offshore in the region west of the Antarctic Peninsula between Livingston Island and south of Marguerite Bay (Waters and Smith, 1992). Each station in the study region is identified with a Palmer grid location, with the first 3 digits being the grid line in km from the base line south of Marguerite Bay, and the second 3 digits being the grid station in km from the base line parallel to the Antarctic Peninsula, e.g. 600.040 is the station on the transect line 600 km north of the 000 line south of Marguerite Bay running on/off shore and 40 km seaward of the 000 line running alongshore next to the continent. The first summer (January – February) cruise for the Palmer LTER was in 1993. The mesoscale grid occupied during that cruise has been surveyed each subsequent summer. This study analyzed data through the summer of 2004, creating a 12-yr time series. The summer study region (PAL grid) was between Anvers and Adelaide Is., and included the 200 to 600 transect lines (see Fig. 1). Islands interfered with the exact spacing of the inner coastal stations, but selected stations representative of the Grandidier Channel (inner 600 and 500 lines), behind the Biscoe Islands (Renaud Is north of Lavoiser Is, inner 500 and 400 lines) and inside Crystal Sound (inner 400 and 300 lines) have been occupied whenever ice

conditions have allowed. Sampling was conducted from the MV *Polar Duke* from 1993 through 1997 and with the ARSV *Laurence M. Gould* from 1998 through 2004. Cruises are identified with year and month of start, e.g. '93Jan'. Not all stations were sampled on all cruises, due to weather, ice or scheduling issues (Table 1).

2.2. Sample collection and analysis

Zooplankton and micronekton were collected with a 2 x 2 m fixed-frame net (~ 700 μm knotless nylon square mesh, 500 μm mesh cod end) towed obliquely between the surface and 120 m as described in Quetin and Ross (2003). The depth chosen for these standard tows was based on evidence that aggregations of krill were seldom found below 120 m in the summer in this region (Ross et al., 1996). Acoustic transects during each tow suggest that the bulk of the biomass of the macrozooplankton is also above 120 m, and that consequently we have captured spatial patterns in biomass for the other 4 species in the PAL grid during summer (unpublished data). The volume of water filtered was measured with a General Oceanics flowmeter mounted in the net frame. Standard tows were centered on Palmer LTER grid locations, and lasted for about 30 min at ship speeds of 2.0 to 2.5 kts (3.7-4.6 km h^{-1}).

Once the catch was on board, the contents of the cod end were gently poured into seawater in a large (50 liter) tub, and the catch sorted live. We identified, counted, and measured the wet volume of the macrozooplankton. For this study we focused on the numerical dominants (~ 97% of the total calculated over the PAL grid for the 12 yrs of the study) of the species ≥ 2 mm collected quantitatively with the 2-m net: three euphausiids (*Euphausia superba*, , ~ 22%; *E. crystallorophias*, ~ 4%; *Thysanöessa macrura*, ~ 46%), one salp (*Salpa thompsoni*,~ 10%), and one pteropod (*Limacina helicina*, ~15%).

The zooplankton catches also included other species of macro- and mesozooplankton ≥ 2 mm: amphipods (*Themisto gaudichaudii* and other species), 2 other species of euphausiids (*E. frigida* and *E. triacantha*), chaetognaths, other pteropods (*Clione spp* and *Clio pyramidata*), tomopterid worms, other polychaete worms, siphonophores, ctenophores, medusae and larval fish. Analysis of these minor taxa (in biomass and numbers) was beyond the scope of this study. Large catches were split, and the split factor determined by the ratio of total volume to the volume identified and counted. After identification and counting, either the entire catch or the subsample was preserved in 10% formalin buffered with marble chips. Smaller mesozooplankton (< 2 mm) such as copepods and zooplankton living somewhat deeper in the water column were collected at the same stations with a 1-m fixed frame net of 333 μm mesh fished obliquely to 300 m. Results from these tows are outside the scope of this study.

Counts of subsamples were adjusted by the split factor before standardizing the abundance to the volume of seawater filtered, and performing any statistical analyses. For most tows, the split factor was estimated for individual species and was less than 5, i.e. at least 20% of the total catch of a species was counted. Data on the abundance of zooplankton are characterized by the presence of a finite number of zero values, a lognormal distribution of the non-zero values, and a high variance in the log distribution of the non-zero values, called a delta distribution (Aitchison, 1955). For zooplankton data, estimates of the mean and variance based on the delta distribution are better than the ordinary sample mean (Pennington, 1983; Gilbert, 1987). The delta distribution estimate of the mean and variance was utilized twice, first for the annual mean, and again for the climatological mean. The following equations were used to calculate the mean (c) and variance (var_{est} (c)) of abundance data with a sample size of n, and m non-zero values ($x_1 \ldots x_m$) where y and s_y^2 are the sample mean and variance,

respectively, of the natural log of the non-zero values, and t is half the variance, i.e. = $(s_y^2/2)$:

$c = (m/n) \exp(y) G_m(t)$ when m>1,

$= x_1/n$ when m=1, and

$var_{est}(c) = (m/n) \exp(2y) \{(m/n) G_m^2(t) - ((m-1)/(n-1)) G_m(s_y^2 (m-2)/(m-1))\}$ when m>1,

$= (x_1/n)^2$ when m=1.

The factor G_m is calculated with the following progression, based on m and s_y^2,

$G_m(t) = 1 + ((m-1)\,t)/m + ((m-1)^3 t^2)/(2!\, m^2 (m+1)) + ((m-1)^5 t^3)/(3!\, m^3 (m+1)(m+3)) + \ldots$

and can also be found in the tables of Aitchison and Brown (1969).

Each abundance estimate also had an associated time of sampling in year days, and a Palmer grid line and grid station location. The means and variances for each grid cell and each year were inspected for extremely high variances that indicated a disproportionate influence of a single tow (flier) on the means. We define a single tow as a flier if the absolute variance is driven by that one estimate, and that one estimate is an order of magnitude greater than the next highest estimate. Three estimates of abundance for *Euphausia superba* were eliminated based on these criteria, one each in 1993, 1998 and 2002. No estimates from the other 4 species met the criteria.

2.3. Analysis of species abundance data

The study region was divided into 50 equal areas with dimensions of 100 km alongshore, centered on gridlines 600, 500, 400, 300 and 200, and 20 km on/offshore, centered on gridstations 000, 020, 040, …, 200 (see Fig. 1). The isobaths on all figures are

for 450 m, 750 m, and contoured at 1500 m intervals at depths > 750 m. Three regions defined by their temperature/salinity characteristics (Martinson et al., this volume) are indicated on the climatology and trend figures: coastal, essentially < 300 m except the area of Marguerite Bay just south of Adelaide Is.; shelf, from the coastal stations to the 750 m isobath; and slope, > 750 m. The inner shelf is from stations 040 to 100, and the outer shelf from station 120 to the 750 m isobath.

2.3.1. Climatologies and anomalies

Climatologies are the mean values (as defined above for delta distribution data) of the abundance of the 5 zooplankton species, and yearly anomalies represent the deviation from the climatological mean for a specific year. Climatologies were calculated for each grid cell by averaging all values within a grid cell for a single year with the delta distribution, and then averaging all of the yearly averages within the cell for the overall mean, again with the delta distribution. The color scales for the climatologies and anomalies are logarithmic, with expanded lower ranges. Units are individuals (ind) 1000 m^{-3}. The anomaly plots are based on the difference between the climatological mean and the annual mean, calculated for the non-linear delta distribution as in Pennington (1983), thus the sum of the anomalies would not necessarily be zero. Warm colors (yellow/red) indicate areas where the abundance in a particular year was greater than the long-term mean (positive anomaly), and cool colors (green/blue) indicate areas of negative anomaly.

By plotting the 12-yr climatology for each species on figures with isobaths and regional divisions, we can see the mean spatial pattern of abundance in relation to depth contours, water mass distribution and the islands near the coast. The anomaly plots allow one to see if interannual variability in abundance, as shown by the deviation

from the climatology, is greater in one part of the PAL grid than another or tends to be positive in some areas/years and negative in others. Inspecting the series of anomaly plots allows one to detect if there are patterns, trends or shifts in pattern of positive or negative anomalies throughout the time-series, either in positive/negative years overall or in specific regions. Timing of these cycles or trends or shifts can then be correlated with other concurrent events either in the PAL grid or more globally.

2.3.2. Principal Components Analysis

Additional insight into the interannual variability and its spatial structure was obtained via Principal Components Analysis (PCA). Conceptually, (see *Martinson et al.*, this volume for full details), PCA works with a covariance matrix, describing the covariability between time series as a function of grid location. This matrix captures the variability (about the climatology) throughout the grid. PCA decomposes this matrix so as to produce a set of "modes" (consisting of spatial patterns of the data, and corresponding time series, that describe how the patterns change their amplitude through time). The amplitude of a mode's spatial pattern at any time is determined by multiplying the spatial pattern at each grid point with its amplitude at that time. The modes are orthogonal, each describing a known fraction of the total variance. They can be added together to recreate the original data distribution (in space, and in time). Ideally, a complex dataset in space and time can be decomposed into a few modes capturing most of the variance and related to forcings or other variables of interest. Subtle variants of the method allow one to isolate covarying modes between different variables.

Construction of the covariance matrix is hindered by gaps in the data that occur due to weather problems, gear malfunction or ship time limitations and thus it is necessary to estimate the sample covariance matrix. The sample covariance matrix was obtained from the anomaly time series in the grid, quantifying how the data co-vary in space and time across the sampled domain. The empirical orthogonal function (EOF) structure was calculated from the sample covariance matrix, representing a physically-consistent basis for the observations, where the lower order EOFs represent spatially-coherent structures whose shapes are preserved through time. The time-varying amplitudes of the full modal structure of EOFs were then calculated; these are the principal components (PCs), the temporal variance of the EOFs. Data gaps were filled, when necessary, following the reduced-space optimal analysis (OA) of Kaplan et al. (1998). This data-adaptive method produces a smoothly interpolated data set that best preserves the coherent spatio-temporal structure inherent in the data (Martinson et al., this volume).

The PCA analysis (with climatology removed) is designed to isolate signal from noise, and detects a sequence of modes that each capture a defined percent of the spatial co-variance in time. However, like all such methods, this methodology will produce modes even for pure noise. We anticipate that modes describing the most total variance represent signal, assuming that the signal would occur in a coherent manner, whereas modes accounting for very little variance (or variance concentrated in isolated locations) represent noise. Thus, we need to match modes (their variation in time and/or their spatial patterns) to features that we expect control or otherwise impart some influence on the spatial and/or temporal distribution of the data being decomposed. For example, we might find a mode whose spatial pattern shows a seemingly arbitrary pattern across the grid, but its temporal variability may closely co-vary with a climate signal (e.g., El

Niño-Southern Oscillation; **ENSO**) that we expect to be an important driver of the ecosystem. Likewise, if a mode's spatial pattern is similar to the climatology, the variability may be a modulation of the seasonal cycle (providing one avenue to explore regarding mechanisms driving the variability).

We present modes with the EOF (spatial pattern) and PC (time-varying amplitudes) that describe more than about 10% of the variance. The number of modes necessary to account for the bulk of the variance, and the pattern shown by the cumulative percentage with each additional mode varies with different physical and biological parameters, and in this study with species of zooplankton. The color scale for the EOF is related to the magnitude of the negative and/or positive effect in a particular region. A low number would indicate the region is less sensitive to the particular mode. The spatial pattern, i.e. the relative differences in abundance attributed to the mode, is maintained even as the overall magnitude changes. Combining the spatial and temporal (PC, amplitude versus year) characteristics of a mode allows us to detect which regions of the PAL grid are most responsive to the mode and whether the signature in a particular year is negative or positive. The PC also illustrates temporal patterns – random, regular pulses, trends – in a mode and helps identify possible environmental factors (or modes of those factors) that are likely candidates for further testing. The sign of a mode's spatial pattern and time series is arbitrary. Both signs can be changed together so that the product is still the same (e.g., negative amplitude factor times a positive amplitude in space yields a negative amplitude in space for that particular year; reversing the sign of the pattern and time series still yields a negative spatial amplitude). Hence, the signs are often reversed to facilitate comparison to other indices, modes, etc. The presumption is that these spatially-coherent patterns that are consistently found throughout the time-series, albeit with varying amplitudes in a

specific year, may be a result of interactions of the zooplankton species with a physical or biological variable. We understand that variability in distribution and abundance may be driven by multiple variables, and thus would expect to require multiple modes in order to account for the majority of the variance.

2.3.3. Trends analysis

The trend plot for each species shows the slope of the linear regression line of the anomalies in abundance versus time for each cell over the twelve years. The color scale represents the number of individuals per 1000 m^{-3} lost (negative slope) or gained (positive slope) over the time-series. With this plot we can evaluate whether there are linear trends in abundance of the 5 species either over the entire grid or only in specific regions. Any trend, however, that is not linear will not show clearly. Nor will we be able to detect trends involving cycles with a period that is long compared to the length of the data set. The caveats are particularly pertinent for a species like Antarctic krill with a strong 5-6 yr cycle with abundances varying by a factor of 20 within a cycle (Quetin and Ross, 2003), and consequently only 2 complete cycles within the currently analyzed data set.

2.4. Two-variable comparisons

We also conducted a series of 2-variable comparisons of the temporal/spatial distributions of each pair of species to investigate whether any species were closely correlated in space and time. If so, the question is whether the correlation is due to similar physical/biological causes or to species-species interactions. Lastly, we

compared the temporal/spatial distributions of each species to four seasonal sea-ice parameters as described in Stammerjohn et al. (this volume) (Table 2). For the 2-variable zooplankton comparison we used the delta distribution estimates of the means and variance. However, for the comparison of the different zooplankton species to the seasonal ice parameters, we used a log transformation of the number of individuals plus 0.1 1000 m^{-3}, i.e. log [1000*(number+0.1)/(volume filtered in m^3)] to approximate a normal distribution for comparison to seasonal sea-ice parameters.

The two products of this comparison are (1) a heterogeneous correlation map, which gives an r or correlation coefficient for two optimally interpolated time series in each cell over the time of the study, and (2) a spatial correlation coefficient, r, for a comparison of the climatologies of the two parameters, i.e. one pair of values from each grid cell. The heterogeneous correlation map is a plot that shows the location, magnitude and spatial extent of positive or negative correlations, whereas the spatial correlation coefficient refers to the correlation between the two climatologies. Even if the spatial correlation coefficient is low for the overall study region, there may be specific areas appearing on the heterogeneous correlation map where a strong correlation exists, indicating the involvement of more spatially restricted or local processes.

3. Results

In describing the spatial patterns we use the convention that 'northern' refers to the northern PAL grid, encompassing the 500 and 600 lines, 'mid-' is the middle PAL grid, encompassing the 300 and 400 lines, and 'southern' is the southern PAL grid, encompassing the 200 line. We recognize that the orientations are not strictly north and

south since the PAL grid is oriented to the Antarctic Peninsula which is itself oriented on a southwest to north east axis, not a north to south axis.

3.1 Species of macro- and mesozooplankton

The climatologies of the 5 species showed some common features. The abundances were generally higher in the north than the south, independent of any on/off shore gradient. For most species, an on/offshore gradient existed, but for some the higher abundances were inshore, and for others offshore. For *Euphausia crystallorophias*, although the pattern was a band along shore, there were still somewhat lower concentrations in the south. Detailed results follow, moving from species dominating the slope region to the species in the inner shelf and coastal region.

3.1.1. Salpa thompsoni

The climatology for *Salpa thompsoni* showed an "r" pattern, with abundances generally two orders of magnitude higher on the slope and northern shelf regions than on the mid- and southern shelf regions (Fig. 1). In the "r" pattern, also seen in heat flux and winter salt deficit among other physical parameters (Martinson et al., this volume), the abundance/magnitude of the parameter is more or less constant north to south on the slope as delimited by the shelf break (upright of the "r"), and then spreads across the north end of the grid (curve at top of "r"). *S. thompsoni* was rarely present in the coastal region (Fig. 1). Highest abundances (red/orange, 150 ind 1000 m^{-3}) were found in the northern slope region, and lowest (light blue, 0.25 ind 1000 m^{-3}) in the southern shelf region. The variance in abundance was highest on the northern shelf west of Anvers Island and on the southern slope. Variability was particularly low in the mid- and northern coastal regions where *S. thompsoni* was rarely, if ever, found.

The anomalies in the abundance of *Salpa thompsoni* showed a distinct change in pattern during the study (Fig. 2). The first 8 yr of the study (1993 – 2000) were years of extremes, showing either positive (patches of yellow/red) (1994, 1997 and 1999) or negative (primarily light green or blue) (1993, 1995, 1996, 1998) anomalies. The last 4 yr of the study (2001 – 2004) generally appeared not to be years of extremes, but showed anomaly patterns ranging from moderately positive (green/yellow) to relatively high positive (2003) anomalies, particularly on the shelf region from the 500 line south. Two years showed uniform anomalies across the grid; 1999 stood out as a year of high anomalies across the grid whereas 1993 was slightly negative. In 9 of the 12 years, the southern slope region had a strong negative anomaly. Only during the 1999 to 2001 period were anomalies positive in this region.

For *Salpa thompsoni*, the first 7-8 modes captured 90% of the total variance (Fig. 3). The first two modes showed anomaly patterns describing ~ 48% and ~ 11% of the variance in time respectively (Fig. 4 A, B). Mode 1 was driven by the overall anomaly patterns shown in Fig. 2, and described the pulsed abundance across the grid, with the PC > +10 in the 5 'salp' years (1994, 1997, 1999, 2002 and 2004), and PC < –20 in 1993, 1995, 1996, and 1998 (Fig. 4 A, upper panel). Subsequent to 1998, the only year with a negative PC1 was 2000 where the positive anomalies were concentrated in the slope region and not across the grid. The highest response (red) to mode 1 was found in the northern inner shelf and mid-grid slope regions, with moderate response (yellow/green) in the southern slope and mid-grid shelf region (Fig. 4 A, lower panel). Mode 2 reflected the spatial differences in areas of large anomalies from the climatology in the 'salp' years of 1997 and 1999 (Fig. 4 B). In 1999 the anomalies for *S. thompsoni* were moderately high in the southern shelf and coastal regions, and in 1997 they were moderately high in the northern coastal and mid-grid inner shelf regions. In mode 2 the

two major areas of response were (1) in the coastal regions, positive in the south and negative in the north and (2) negative in the northern and mid-regions which combined with a high negative PC in 1997 yielded higher values in the north than the south, and with a high positive PC in 1999 reinforced the positive EOF in the southern shelf and coastal regions (Fig. 4 B, lower panel).

Overall trends in the anomalies in abundance of *Salpa thompsoni* were not present in the shelf and coastal regions during the 12 years of the study (Fig. 5). However, in restricted areas, particularly in the northern slope region, abundances have been increasing at rates of 6 - 14 ind 1000 m^{-3} yr^{-1}, an increase of ~ 5-10% in what are high abundance regions.

3.1.2. Limacina helicina

The climatology of the shelled pteropod, *Limacina helicina*, showed a different pattern than *Salpa thompsoni*. The overall cross-shelf gradient showed a bulge into the mid-grid shelf region, with a peak in abundance (red/orange 100 ind 1000 m^{-3}) along the outer edge of the northern shelf down into the center of the bulge on the 400 gridline. *L. helicina* was either missing or in low (light blue, 3 ind 1000 m^{-3}) abundance in the coastal region north of Adelaide Island, and moderately (yellow/orange 20-60 ind 1000 m^{-3}) abundant on the entire shelf, in the coastal region south of Adelaide Island and in the slope region of the southern part of the grid (Fig. 6). In the southern region, the distribution did not follow a smooth gradient as abundances on the shelf were less than in either the slope or coastal region. The standard deviations were the inverse of the climatology, highest where the abundances were an order of magnitude less, i.e. over the shelf and to the south both over and off the shelf as compared to the mid-grid shelf. This suggests that the areas of high abundance were relatively stable.

The anomalies during the years between 1993 and 1997 showed various patterns with areas of both positive and negative anomalies, with 1993, 1994 and 1998 showing the most extensive and uniformly negative anomalies (Fig. 7). Anomalies have been more uniformly positive in the 6 yr since 1998, with less interannual variability than prior to 1998. In 2002, the anomalies were the highest and widest spread of any year sampled (Fig. 7).

The first 6 modes captured 90% of the total variance for *Limacina helicina* (Fig. 3). The first two modes showed anomaly patterns describing ~ 54% and ~ 12% of the variance in time respectively (Fig. 8 A, B). The area of response (red) for mode 1 covers most of the shelf and coastal regions from south of Adelaide Island to the 500 gridline. Low response (blue) to mode 1 was seen in areas with both the lowest (northern coastal and inner shelf regions) and highest (slope region) abundances. This pattern suggests that the environmental signal for the response reflected in mode 1 is not tied to climatological abundance. The PC1 appeared to be driven by the lack of *L. helicina* in the mid- and southern shelf regions in 1993, 1994 and particularly 1998 (> -15) (Fig. 8A, upper panel). The areas of response corresponded to the anomalies seen in those 3 yrs (Fig. 7 and A, lower panel). Mode 2 accounts for much less of the variance than mode 1 for *L. helicina*, and the areas of strongest response are primarily in the southern region, and of opposite signs for the shelf and coastal regions compared to the slope region (Fig. 8 B, upper panel). The EOF pattern for mode 2 shares many of the features of the 1997 and 2004 anomaly plots (Fig. 7). Although the PC2s were strongly negative in 1993 and 1996, a consistent feature is the decreased variability in the amplitude of PC2 after 1997, i.e. 1998 to 2004 (Fig. 8 B, upper panel).

Over the 12 yr of the study there is a positive trend in abundance of *Limacina helicina* in certain regions of the PAL grid (Fig. 9). The trend is more pronounced in the

northern and mid-grid shelf region, and in the southern slope region, i.e. on the inner edges of the regions of high and maximum climatological abundances (Fig. 9). This pattern means that the range of the population was extending during the period of study, although *L helicina* was still primarily concentrated in the northern region as shown in the climatology (Fig. 9).

3.1.3. Euphausia superba, the Antarctic krill

The climatology for the abundance of *Euphausia superba* in the Palmer LTER study region showed both north/south and on/offshore gradients (Fig. 10), the long-shelf with cross-shelf gradient pattern described for the summer salt deficit (Martinson et al., this volume) and retreat of 15% ice concentration (Stammerjohn et al., this volume) . Broadest regions of high abundance (red/orange, 250 ind 1000 m^{-3}) were generally found in the northern inner shelf and coastal regions, with moderate abundances along the inner shelf/coastal region junction all the way south. In the slope region, abundances were lower (light blue/blue, 15 ind 1000 m^{-3}) in the southern and mid-grid regions, and lowest (dark blue, < 10 ind 1000 m^{-3}) in the far north (600 line). Over the inner shelf, abundance was higher from the mid-point of Adelaide Island north than in the very southern part of the study region at the entrance to Marguerite Bay. The pattern for standard deviations showed that variance was highest in the same areas as the highest abundance.

The anomalies showed a repeated pattern illustrated by the 6 years from 1994 to 1999. The pattern was composed of two initial years with negative anomalies (lower than average abundances) (1994/1995) followed by 2 years of positive anomalies (higher than average abundances) (1996/1997) (Fig. 11). In the 1996/1997 pair there were somewhat higher positive anomalies on the inner 600 gridline than in the

2002/2003 pair. The prevalence of areas of positive anomalies decreased over the next 2 years (1998/1999), with a tendency for positive anomalies in the mid- to southern region (Fig. 11). Of interest was the occurrence of high positive anomalies in 2002 in a region of low mean abundance (Fig. 10) at the mouth of Marguerite Bay in the southern coastal region.

For *Euphausia superba*, the first 9 modes captured 90% of the total variance (Fig. 3). The first two modes showed anomaly patterns describing ~ 21% and ~ 15% of the variance in time respectively (Fig. 12 A, B). PC1 showed two cycles with positive amplitudes in 1996 and 1997, and again in 2002 and 2003 (Fig. 12 A, upper panel), as seen in the anomaly plots. The response was strongest and positive in the northern two-thirds of the grid, with a smaller negative response a feature in the southern region (Fig. 12 A, lower panel). Differing from mode 1, the areas of response for the EOF of mode 2 were primarily on the shelf west of Adelaide Is., and the mid-grid slope region (opposite signs), forming a wedge in the south-southwest corner. PC2 was strongly negative (-15) in 1993, and strongly positive in 2004 (+15), with its amplitude generally trending more positive during the 12-yr study. Overall the suggestion is of a shift toward slightly greater abundances on the southern shelf. The EOF appeared to be primarily a combination of influences in 1993 and 2004, the two years of strongest difference in amplitude.

Overall trends in the anomalies of abundance appear to be low and showed an inconsistent and variable pattern across the PAL grid, implying that there is no overall linear trend in the data to date. There were two patches of consistent decrease, in the coastal 600 line region and west of northern Adelaide Is., as highlighted by mode 2 (Fig. 12 B, lower panel). However, the presence of two cycles complicated the linear trend analysis.

3.1.4. Thysanöessa macrura

The climatology of *Thysanöessa macrura* showed the diagonal-striped pattern described by Martinson et al. (this volume), with lowest abundances (values) in the mouth of Marguerite Bay in the lower right of the grid the radiating up to the northwest corner of the Pal grid with highest abundances on the shelf/slope intersection of the 600 gridline (Fig. 13). *T. macrura* occurred across the northern shelf and down to the mid-grid slope region in high (red/orange, 600 ind 1000 m^{-3}) to moderate (yellow, 150 ind 1000 m^{-3}) abundance, but was in low (light blue, 40 ind 1000 m^{-3}) abundance in the northern slope and southern inner shelf region. *T. macrura* was in lowest (dark blue, <20 ind 1000 m^{-3}) abundance throughout most of the coastal region.

There was a distinct change in the magnitude and sign of the anomalies between 1998 and 1999. Between 1993 and 1998, anomalies were positive (tend to yellow/orange) throughout most of the grid (see 1996, Fig. 14). In the 4 years from 1999 through 2002 anomalies were small in the southern region, but often negative (blue/green) in the northern and mid-grid regions (see 1999 – 2002, Fig. 14). In 2003 two cells with positive anomalies appeared. In 2004 the anomalies were again positive over a large portion of the grid, similar to 1996 (Fig. 14).

For *Thysanöessa macrura*, the first 9 modes capture 90% of the total variance (Fig. 3). The first two modes showed anomaly patterns describing ~ 23% and ~ 18% of the variance in time respectively (Fig. 15 A, B). Mode 1 was driven by the pattern of 1998, leading to the maximum amplitude of PCI in 1998 (Fig. 15 B, upper panel). The area of response for mode 2 was primarily along the shelf break, with a strong localized response on the slope of the 500 gridline (Fig. 15 B, lower panel). PC2 was positive between 1994 and 1998, then negative or near zero between 1999 and 2003, returning to

positive in 2004 (Fig. 15 B, upper panel) as was the anomaly pattern described for 1999-2004. Trends in the anomalies of abundance were near zero over much of the study region. The few positive or negative cells did not form a pattern.

3.1.5. Euphausia crystallorophias

The climatology for *Euphausia crystallorophias* was thelong-shelf with cross-shelf gradients pattern (Fig. 16), as found for the other *Euphausia* species in the study. However, the pattern had steeper gradients in abundance and extended closer to the continent than that of *E. superba*. Maximum (red/orange, > 50 ind 1000 m^{-3}) abundance of the *E. crystallorophias* was restricted to the coastal region, with areas of moderate (yellow/green, 1-10 ind 1000 m^{-3}) to low (light blue, < 1 ind 1000 m^{-3}) abundance in the inner shelf region (Fig. 16). In the far north, *E. crystallorophias* were sometimes found on the outer shelf and slope regions. The variance decreased moving offshore into habitat where the ice krill did not occur.

In general, anomalies in the inner shelf and coastal areas are of more significance to the pattern of distribution of *Euphausia crystallorophias* due to the rarity of positive catches of this species in the outer shelf and slope regions. Occasional small areas of high variance in these seaward regions merely suggest that at some time and under some conditions *E. crystallorophias* can be found across the grid. However, these spots tended to be due to a single catch of low numbers combined with zeroes in the other years, yielding a high variance. Thus we restrict our discussion of the anomaly pattern to the inner shelf and coastal regions of the PAL grid, as outlined in dark blue (Fig. 17). Years with predominately negative anomaly patterns (1995, 1998, 1999, and 2001) contrasted years with predominately positive anomalies (1996, 1997, 2002, and 2004). In 1998, negative anomalies occurred throughout the inner shelf and most of the coastal

regions, whereas in 2004 equal in magnitude but positive anomalies occurred over most of the inner shelf region (Fig. 17). Behind the Biscoe Islands (~ 500.000 and 400.000), with some of the highest abundances of the coastal region (Fig. 16), there were positive anomalies in 1997. Anomalies on the inner shelf did not necessarily follow the pattern of the coastal region, e.g. 1996.

For *Euphausia crystallorophias*, the first 9 modes captured 91% of the total variance (Fig. 3). The first two modes showed anomaly patterns describing ~ 26% and ~ 15% of the variance in time respectively (Fig. 18 A, B). The areas of response for mode 1 were primarily in the inner shelf and coastal areas of the northern and mid-grid regions, and an isolated area just west of Adelaide Is. (Fig. 18 A, lower panel). After 1995, the between-year changes in the magnitude of PC1 increased greatly (Fig. 18 A, upper panel). The areas of response for mode 2 were the mid-grid coastal and southern coastal regions, but of opposite sign (Fig. 18 B, lower panel). Mode 2 incorporated the variability just west of Adelaide Island, positive in 1996, 1998, 1999 and 2004, and negative in 1995, 1997 and 2002. The combination of mode 1 and mode 2 determined the anomaly observed just west of northern Adelaide Is. in any one year. Most slopes in the trend plot were around zero, with a few positive cells in the northern coastal region driven by catches in the last two years of this analysis. More data will be required to determine if this recent increase is part of a longer-term trend.

3.2. Spatial Correlations

3.2.1. Species to species

The spatial correlation coefficients for the climatologies of the species pairs were not strong (Table 3), reflecting the distinct differences in the climatological abundance

patterns of their spatial distributions. The only spatial correlation coefficient ≥ 0.5 was between the two *Euphausia* species (+0.54), suggesting some overlap in their distributions. The habitat of the *E. crystallorophias* was primarily restricted to coastal and inner shelf waters, and the spatial correlations of its distribution with the two species with higher abundances primarily in sloe and shelf-break areas (*Salpa thompsoni* and *Limacina helicina*) were low, -0.17 and -0.29, respectively. The habitat of the other two euphausiids, *E. superba* and *Thysanöessa macrura,* was primarily shelf and slope, although shifted relative to each other, giving another low correlation (-0.12). The spatial correlations of *E. superba* and *T. macrura* with other species were also relatively weak, all < 0.43, with the weak and positive spatial correlation coefficients reflecting partial overlap in the respective distributions of the two species. Of particular interest was the lack of a moderate or strong spatial correlation coefficient (either negative or positiv) between *E. superba* and *S. thompsoni* climatologies (-0.15). On average the climatologies of *E. superba* and *S. thompsoni* were not correlated. The time series regression for each grid cell also showed relatively weak correlations (r < 0.4) in 46 of the 50 cells, indicating that even in areas of overlap in the two distributions there was little relationship between the anomalies in abundance of these two species.

3.2.2. Species abundance to sea-ice parameters

Correlations between the climatological abundance of the 5 zooplankton species in January and climatological seasonal sea-ice parameters for each grid cell varied with the distribution of the species. The spatial distributions of *Salpa thompsoni* and *Limacina helicina*, offshore species, and *Euphausia crystallorophias*, a coastal species, were most closely correlated with the 4 sea-ice parameters ($r^2 > 0.42$ for sea-ice advance, retreat and days), whereas the abundances *Thysanöessa macrura* and *E. superba* were either not or

only moderately correlated (Table 4). Ice persistence was the variable with the lowest correlation coefficients overall (Table 4).

Heterogeneous correlation maps showed the within-cell correlations of a zooplankter and sea-ice parameters. Here we present selected heterogeneous correlation maps that correspond to high correlation coefficients or are pertinent to specific questions. The abundance of *Salpa thompsoni* was negatively correlated (-0.5 to -0.6) with the number of ice days the previous year over most of the slope and shelf regions (Fig. 19). With a long duration (ice days) and a late retreat of sea-ice, few salps were found on the shelf in January (Fig. 19, Table 4). For *Limacina helicina,* the abundance in a grid cell was also negatively correlated (-0.5 to -0.6) with the number of ice days the previous year, but this negative correlation was restricted to the southern and mid-shelf regions and parts of the slope region where the abundance of *L. helicina* was at a maximum (Fig. 20, compare to Fig. 6). In the northern inner shelf and coastal region the abundance of *L. helicina* was not related to ice days.

Although, generally, the spatial correlation coefficients of *Euphausia superba* and the various sea-ice parameters were weak (<0.15) (Table 4), the heterogeneous correlation map with ice persistence showed isolated areas of positive correlations (+0.6) in regions where in specific years the catches of *E. superba* have been high, e.g. just west of Renaud on the 500 gridline and at the seaward end of the 400 and 600 gridlines (Fig. 21). For *E. crystallorophias*, the heterogeneous correlation map with ice retreat suggested that *E. crystallorophias* was more apt to be found in the regions just west of Renaud Is. on the inner shelf and just south of Adelaide Is. on the inner shelf when ice retreat was later in the spring (Fig. 22). These regions did not show high abundance in the climatology, but were highly variable.

4. Discussion

Few studies of epipelagic zooplankton assemblages have been conducted in summer in the Palmer LTER study region, oriented primarily to the shelf and coastal zones mid-way down the relatively broad shelf of the western side of the Antarctic Peninsula. For the U.S. portion of Southern Ocean GLOBEC, the focus was on austral fall and winter surveys and processes in the Marguerite Bay and the proximate continental shelf (Hofmann et al., 2004), an area that overlaps the southern end of the PAL grid. Although waters west of the Antarctic Peninsula and south of the SBACC belong primarily to the seasonal pack-ice zone, previous studies in spring and summer to the north and west have shown that these waters can contain species from both oceanic (generally warmer water with depths > 2000 m) and shelf/break and slope zooplankton assemblages (Siegel & Piatkowski 1990; Smith & Schnack-Schiel 1990; Schnack-Schiel and Mujica, 1994; Ward et al., 2004). The major herbivores (copepods, euphausiids and salps) often dominate in different regions (Voronina, 1998; Ward et al., 2004), but can be found in mixtures in transition zones.

As previously seen in studies of zooplankton communities at the tip of the Antarctic Peninsula and in the Scotia Sea (c.f. references above and in Ross et al. 1996), the 5 macrozooplankton species in this study occupied different biomes, e.g. slope (oceanic influence) versus shelf versus coastal (cold continental) zonesIn the PAL LTER study region from 1993 through 2004, *Salpa thompsoni* and *Limacina helicina* dominated the deeper waters of the slope region, and *Euphausia superba* and *Thysanöessa macrura* dominated in the shelf region. *E. crystallorophias* was the dominant zooplankter in the coastal waters next to the continent that are more likely to have lingering summer sea-ice (Stammerjohn et al., this volume). Although there were distinct climatologies for the

5 species, there were also significant overlaps in the climatological distributions, with more or less overlap depending on the year, indicating that the different species could co-occur in transition zones.

Overall abundances of the macrozooplankton species in this study were in the mid-range of previous studies in the southwest Atlantic. During the survey sponsored by the Commission for the Conversation of Antarctic Marine Living Resources (CCAMLR) – the CCAMLR 2000 Survey - average abundance of *Salpa thompsoni* was 84 ind 10^{-3} m^{-3} (Kawaguchi et al., 2004). In the same survey Ward et al. (2004) documented mean abundances of *S. thompsoni* north and south of the SACCF as 37 and 119 ind 10^{-3} m^{-3} respectively. In this study, the climatological abundance for *S. thompsoni* in the northern slope region, the region of maximum abundance, was 150 ind 10^{-3} m^{-3}, similar to the recent abundance estimates from CCAMLR 2000 and within the range of earlier studies at the northern tip of the Antarctic Peninsula (3.8 - 110.7 ind 10^{-3} m^{-3}) (Kawaguchi et al., 2004). Ross et al. (1996), in a review, stated that *Limacina helicina* can occur at abundances greater than 50 ind 10^{-3} m^{-3}. More recently, Ward et al. (2004) documented mean abundances of *L. helicina* north and south of the SACCF as 16,669 and 130 ind 10^{-3} m^{-3}, respectively. In the PAL grid, abundances ranged from 20 – 60 10^{-3} m^{-3} in regions of moderate abundance and over 100 10^{-3} m^{-3} in regions of high abundance. The abundances appear to generally decrease moving from the oceanic realm to the coastal region.

West of the Antarctic Peninsula, multiple previous studies have documented abundances for both *Euphausia superba* and *Thysanöessa macrura*, but less is known of *E. crystallorophias*. Abundance estimates of *E. superba* range from highs of ~ 2000 10^{-3} m^{-3} in the South Georgia/Scotia Sea region to more moderate abundances of 100 10^{-3} m^{-3} west of the Antarctic Peninsula (Atkinson et al., 2004). At the tip of the Antarctic Peninsula,

abundances of *E. superba* have ranged from maxima of 1,681 ind 10^{-3} m^{-3} in the early 1980s to a low of 9 ind 10^{-3} m^{-3} in 1999, with more recent values of over 200 ind 10^{-3} m^{-3} (Siegel et al., 2002). The climatological abundances within the habitat of *E. superba* in this study ranged from over 300 ind 10^{-3} m^{-3} just south of Anvers Is to less than 10 ind 10^{-3} m^{-3} in the mouth of Marguerite Bay, illustrating mesoscale (50 – 200 km) variability in abundances within the presumed habitat. The smaller *T. macrura* is generally more abundant than *E. superba*, with relative abundances of 452 versus 17 ind 10^{-3} m^{-3}, respectively, north of the SACCF, and 197 versus 39 ind 10^{-3} m^{-3}, respectively, south of the SACCF in the recent study of Ward et al. (2004). In the PAL grid, regions of maximum climatological abundance for *T. macrura* contained 600 ind 10^{-3} m^{-3}, with lows in the coastal zone of < 20 ind 10^{-3} m^{-3}. Siegel and Harm (1996), in a study of the pelagic zone of the Bellingshausen Sea into the pack-ice zone, found abundances of *E. crystallorophias* averaging 2.1 ind 10^{-3} m^{-3}, similar to those found in the Weddell Sea, and slightly lower than those found in the BROKE study region off East Antarctica (80° – 150°E) (Hosie et al., 2000). In the PAL grid, the climatological abundances of *E. crystallorophias* in the coastal zone were considerably higher, i.e. > 50 ind 10^{-3} m^{-3}, with abundances closer to those in the BROKE study and the Weddell Sea on the inner shelf.

4.1. Patterns in climatologies and anomalies

One reason for focusing on patterns in the climatologies and anomalies is that consistencies in pattern may suggest a geographic linkage controlling or influencing all of the variables displaying the pattern. Such coherence helps us focus our investigations on particular mechanisms, i.e. the same mechanism may be attached to specific patterns. One of the major findings of simultaneous analysis with the same approach of the time-series analysis of the biological and physical data collected by the

Palmer LTER group is that all the climatologies fall into one of a group of 4 – 5 patterns (Summary Chapter). The correspondence in patterns infers either common causality or a direct interaction. These findings will allow us to formulate and refine hypotheses that will be tested in further analyses. For several of the zooplankton species the climatologies corresponded to patterns found in other parameters. For example, the climatology of *Salpa thompsoni* is shaped like a small r, the "r" pattern (section 3.1.1), which is also common in physical parameters. Both the winter-average ocean sensible heat flux and the winter salt deficit also show the "r" pattern (Martinson et al., this volume). Does heat flux impact the distribution and abundance of *S. thompsoni* either through its effect on sea-ice cycles or is the effect transmitted through the effect of the heat content on the physiology of the species? A second pattern, long-shelf with cross-shelf gradients was common in both biological and physical variables: *Euphausia superba* and *E. crystallorophias,* summer salt deficit (Martinson et al., this volume), integrated primary production (Vernet et al., this volume), and ice retreat (Stammerjohn et al., this volume). The existence of these gradients both on/off shore and alongshore appears to be a consistent feature of the physics and biology. Perhaps ice retreat is the common driver? Given the coherence in the patterns for *E. superba* and integrated primary production we would predict that growth rates will be higher on the inner shelf than the slope, given the dependence of growth on food availability (Ross et al., 2000; Atkinson et al., 2006). In a third example, both ice advance and *Thysanoëssa macrura*, share a diagonal striped pattern radiating up from the mouth of Marguerite Bay in the lower right of the grid to the upper left. But in this case, the spatial correlation between this euphausiid species and ice retreat is only moderate (Table 4), leading us to suspect a more complex process than that postulated for ice retreat and *E. crystallorophias* (Section 4.6) underlies this distribution pattern. The next step in the

analysis of these data on physical and biological variables that share patterns in space and time will be to investigate linkages and the possible processes underlying the linkages through 2-variable comparisons and cross-correlation analysis. .

The anomaly plots showed that the patterns of interannual variability varied species to species. The anomaly patterns for two species from the same habitat did not necessarily resemble each other, suggesting that the mechanisms underlying interannual variability were not the same for any of the 5 species. However the change in pattern in or after 1998 was detected in several species (Section 4.3).

4.2. Patterns of variance and modes

This analysis of spatial-temporal variability in distribution and abundance of the dominant macrozooplankton species in the Palmer LTER study region revealed several differences among the species, the first of which appears to be associated with life-history characteristics. First, the shape of the cumulative percent of the variance accounted for with increasing number of modes (Fig. 3) was not the same for all 5 species. For the two species commonly characterized as occupying the more oceanic habitat and found in high abundances in the slope and outer shelf of the PAL grid, *Salpa thompsoni* and *Limacina helicina*, mode 1 accounted for over 45% of the variance, and all modes thereafter accounted for much less variance. For all three species of euphausiids, which have longer life spans than the oceanic species, modes 1 and 2 were of similar magnitude, and together accounted for ≤ 42% of the variance. This difference in the shape of the cumulative percent curve (Fig. 3) suggests that the mechanisms driving the variation in the space/time distribution of the more oceanic and shorter-lived species is less complex and more direct than those for the euphausiids. The abundance and distribution of species with 1-2 yr life cycles may be dominated by environmental

conditions of a single year or season or by fewer environmental variables, as suggested by the amount of variance in mode 1 and the smaller number of modes necessary to account for the variance. For the euphausiids that live 4-6 yr, the abundance and distribution are integrating environmental conditions over a longer time span or multiple environmental factors operating on different life stages, as suggested by the greater number of modes necessary to account for the variance. In the case of *Euphausia superba*, we know that there are several critical periods during the life cycle, with different environmental factors impacting the production or survival of the animals during those periods. Thus the distribution and abundance in any one year is the integration of recruitment processes occurring over the previous 6-7 yr.

For three of the species, *Salpa thompsoni*, *Euphausia superba* and *E. crystallorophias*, mode 1 represented the high interannual variability in abundance of the species. In *S. thompsoni*, mode 1 reflected the years when salps were found throughout the shelf and in increasing abundance throughout the PAL grid, and were not restricted to the slope of the PAL grid and the shelf of the 600 gridline (the "r" pattern). Mode 1 for *E. superba* reflected the 6-yr cycle of episodic recruitment found in this species in this region (Quetin and Ross, 2003). Each cycle included two peaks in recruitment success. Episodic recruitment for *E. superba* has been correlated with sea-ice dynamics and to moderate phases of the Southern Oscillation Index (ENSO) cycle (Quetin and Ross, 2003).

4.3. Anomalies associated with 1998, and possible links to the Southern Oscillation Index

Often a mode was dominated by the variance in either one or two years (Table 5). This was more often true of high-level modes than low-level modes, but in two cases (*Limacina helicina* and *Thysanöessa macrura*) mode 1 was dominated by the anomaly

pattern of 1998. The 1998 year had significant anomalies for several species, and marked a change in the pattern of anomalies for others. For *Salpa thompsoni*, since 1998 there have been consistently positive anomalies. Also for both *L. helicina* and *T. macrura* the anomaly pattern changed after 1998, and was steady throughout the following 3 years of prolonged La Nina conditions. For *Euphausia crystallorophias*, 1998 was a year with unusual anomalies. For *E. crystallorophias*, the strong negative anomaly in 1998 throughout the inner shelf and coastal regions was followed by a period of relative instability as the interannual variability in the magnitude of PC1 increased. At the tip of the Antarctic Peninsula, 1998 also marked a change in species composition, likely due to lack of faunal input through advection from water masses to the north (Lipsky, 2005), coincident with a regime shift in the North Pacific and possibly changes in the teleconnections with the western Antarctic Peninsula. For *E. superba* high concentrations were found near the mouth of Marguerite Bay only in 2002, the summer following anomalous atmospheric conditions in the spring of 2001 that had indirect effects lasting into summer (Massom et al., 2006).

The changes in the anomaly patterns coincided with the rapid transition from the very strong El Nino (negative ENSO) conditions of 1997/1998 to La Nina (positive ENSO) conditions in the austral summer of 1998. ENSO remained positive for most of the following three years. For the longer-lived species, whose abundance does not change dramatically on time scales of a few months, the consequence of the anomalous conditions in 1998 may have been a mesoscale-scale shift in distribution, perhaps due to changes in current patterns, in response to the strong teleconnection of the western Antarctic Peninsula region to ENSO, such as postulated for an anomalous year in the 1980s in the Scotia Sea (Priddle et al., 1988). The subsequent change in the pattern of anomalies may be a result of achieving a different equilibrium under stable positive

ENSO conditions over of the next several years after such a strong El Nino. The response to ENSO or other longer-period climate changes may be direct, e.g. water with certain characteristics may shift geographic position year to year (as described in Martinson et al. this volume), bringing with it either the species itself or favorable conditions for one species to develop more quickly than another, or indirect, e.g. changes in sea-ice advance or retreat change conditions for phytoplankton production and thus the species for whom the resulting the food environment is favorable.

4.4. Trend Analysis

One of our goals was to use the anomaly and trend plots to distinguish among interannual variability, cycles, shifts and trends in macrozooplankton distribution and abundance, a goal only possible with the use of a long-term data set. The anomaly plots were useful to detect major shifts in pattern, such as occurred in 1998, or for cyles. A trend, whether over the entire PAL grid or localized, could be detectedin the anomaly plots, perhaps as consistent and decreasing negative anomalies for the first half of the study and consistent and increasing positive anomalies for the second half of the study. But linear trends are more easily seen in the trend plots, where the linear slope of anomalies versus year yields a sense of the magnitude of change in a grid cell or region.

The first detailed map of the spatial distribution of *Salpa thompsoni* in the Southern Ocean (Foxton, 1966) suggested that the southern limit of the distribution was shaped by the ice-edge, with dense concentrations between 45° and 60°S. Recently Pakhomov et al. (2002) re-constructed the map of *S. thompsoni* distribution with data available from 1980 to 1998. There were distinct changes. During the past two decades *S. thompsoni* has been found regularly at high latitudes, and the belt of dense concentrations has extended further south to ~ 65°S. The extension to 65°S is consistent with our

climatology for *S. thompsoni*, which occurs on the 600 gridline south of Anvers Is. at > 64°S nearly every year. The anomaly pattern for *S. thompsoni*, a sequence of 5 years with positive anomalies on the shelf post-1998 after 6 years with only 2 years with positive anomalies on the mid-grid and southern shelf, suggested a possible change in the frequency of years in which *S. thompsoni* was found on the shelf south of 65°S. Pakhomov et al. (2002) suggested that *S. thompsoni* has thermo-physiological limitations that have prevented their appearance at higher latitudes. In the PAL grid, the change in pattern corresponds to the rising heat content of the shelf, which has been steadily increasing since at least the inception of the Palmer LTER (Martinson et al., this volume). However, in the trend plot, although all the slopes were positive, they were small, suggesting caution with a conclusion that salps are increasing in the Palmer LTER study region.

Limacina helicina was the sole species in which there appeared to be a relatively strong positive trend, but the increase was restricted to a band about 70 km wide bordering the highest abundances in the climatology. The range of *L. helicina* appears to be expanding onto the shelf and toward the southern grid from the stable high-abundance region shown in its climatology. In addition, the year in which the maximum heat content of the shelf was observed was also the year with the highest positive anomalies in *L. helicina* (2002, Martinson et al., this volume; Fig. 7). As cited in Pakhomov et al. (2002), Grachev (1991, in Russian) suggested that the southern limit of mass development of the genus *Limacina* is the northern limit of the seasonal pack ice and its associated subsurface cold-water layer. This suggests there may be a mechanism underlying the link between anomalies in *L. helicina* distributions and the heat content of the shelf. Both the species for which possible trends were detected have life spans < 2 yr, and thus potentially there will be a shorter time between

environmental change and population response. For the longer-lived species, due to demographic lags in response, a longer data set or a different type of analysis will be necessary to detect trends clearly (as opposed to cycles).

4.5. Salps versus Antarctic Krill – Salpa thompsonsi versus Euphausia superba

In the PAL grid, *Salpa thompsonsi* and *Euphausia superba* often dominate the total macrozooplankton biomass in the epipelagic layer. During the summer cruises for the Palmer LTER from 1993 - 2004, *S. thompsonsi* and *E. superba* accounted for over 50% of the volume in 62% of the tows, and for over 70% in 48% of the tows in the upper 120 m of the water column (Ducklow et al., 2007). *S. thompsonsi* and *E. superba* were found in the same catch in nearly half the tows, irrespective of the depth of the water (Ducklow et al., 2006).

Co-occurrence of *Salpa thompsoni* and *Euphausia superba* over a large spatial scale as found in some years in the PAL grid is unusual. In most other regions there is a relatively distinct demarcation in the habitats of these two species (Loeb et al., 1997; Voronina, 1998; Nicol et al., 2000; Pakhomov et al., 2002; Atkinson et al. 2004), although in the recent large-scale CCAMLR 2000 study, considerable overlap was also found in the distributions of the two species (Kawaguchi et al., 2004). In the early 1990s, Hofmann and Huntley (1991) suggested that salps were abundant in years following strong El Nino events. During El Nino events, the 'oceanic' community, represented by *S. thompsoni,* would dominate areas where the shelf and shelf-break community, represented by *E. superba*,would normally dominate. Initially this concept was supported both by early results from the Palmer LTER (Ross et al. 1996, 1998) and results from the AMLR research program in the Elephant Island area (Loeb and Siegel 1993, 1994). With the entire 12-yr time series from the Palmer LTER, however, there

does not appear to be as strong a correlation as previously proposed. Although the 1994, 1997 and 2002 'salp years'were near El Ninos, the maximum 1999 'salp year' was during the prolonged La Nina period that lasted from early 1998 until early 2001. Throughout this prolonged positive ENSO period, the anomalies remained moderately positive, i.e. there were more *S. thompsoni* across the shelf than is true for the climatology. The critical physical variable may be the heat content of the shelf, which may have been influenced by the ENSO cycle prior to the present regime of steadily increasing heat content. Also in the region west of the Antarctic Peninsula, the SBACC comes closer to the shelf break than in most of the Southern Ocean, which may foster mixing of the two assemblages.

In an earlier investigation of the relative distributions of *Salpa thompsonsi* and *Euphausia superba*, Loeb et al. (1997) suggested that *S. thompsoni* is a direct competitor with *E. superba* for food, and therefore reproduction in *E. superba* would less successful when *S. thompsoni* is abundant. Kawaguchi et al. (1998, 1999) and Quetin and Ross (2001) used two different approaches to test this idea. Kawaguchi et al. (1998) found no correlation between *S. thompsoni* densities and the 'greenness' of *E. superba*, indicating that they were well fed despite the presence of their potential competitor, and that 'greenness' was tightly correlated to the size of the phytoplankton cell in the water (Kawaguchi et al., 1999). In a 7-yr study, Quetin and Ross (2001) found that reproductive output in Antarctic krill was not correlated with the presence or absence of *S. thompsoni*, but with the timing of spring ice and annual primary production. In the present study, the correlation coefficient for the 12-yr time series was very weak between *E. superba* and *S. thompsoni*, supporting the concept that its abundance is not a predictor of *E. superba* abundance in this region.

One alternative that has yet to be explored in detail is direct feeding by *Salpa thompsoni* on the embryos and larvae of *Euphausia superba* (Siegel, 2005). However, particularly for the embryos the depth ranges of the embryos and *S. thompsoni* may not strongly overlap because the embryos sink rapidly out of the surface layers (Quetin and Ross, 1984). However, the populations may be responding to the same environmental factors, but on different time scales. One of the confounding factors is the difference in the life spans of these two species. Although some of the same environmental factors (seasonal sea-ice dynamics) foster both the development of blooms of *S. thompsoni* and affect recruitment success and abundance in *E. superba*, they operate over significantly different time scales, less than a year for *S. thompsoni* with their annual life cycle, and over multiple years for *E. superba*.

4.6. Correlation with Sea-ice Parameters

Sea-ice plays a role in the development of the distribution pattern of zooplankton because the marginal ice zone acts both as a frontal system with enhanced primary production and a delimiter of cold surface water. The spatial/temporal distribution of *Salpa thompsoni* and *Limacina helicina* (two oceanic species) and *Euphausia crystallorophias* (cold continental shelf species) showed correlations with sea-ice parameters. These are the species' groups that would be most likely to have life history strategies adapted to little ice or summer ice, respectively. We found a strong negative correlation between *S. thompsoni* abundance on the shelf in the summer and the number of ice days in the previous year, similar to the correlations found by Siegel and Loeb (1995) between *S. thompsoni* abundance and ice concentration in winter (negative) and duration of ice-free conditions (positive) at the northern tip of the Antarctic Peninsula. This result is consistent with the original suggestion that the southern limit of the *S. thompsoni* range

was shaped by the ice edge (Foxton 1966), and suggested that a prolonged sea-ice season does not create environmental conditions that would promote a bloom of *S. thompsoni* on the shelf by January. The data in this study were consistent with the concept that seasonal sea-ice dynamics were associated with whether or not *S. thompsoni* was found spread across the shelf, whether due to direct effects of temperature or indirect effects on the timing and size composition of the phytoplankton bloom. Since the first mode for ice days is correlated with the ENSO cycle (Stammerjohn et al. this volume), one might have predicted that *S. thompsoni* distribution would be correlated with the ENSO cycle. However, the change in the pattern of anomalies after the strong El Nino of 1997/1998 suggests that additional aspects of the environment or perhaps the timing of the bloom affect the presence of *S. thompsoni* on the shelf in January. A winter with a shorter ice duration may be only one of the possible sets of conditions that would lead to optimal conditions of phytoplankton composition and concentration for rapid growth of salps in shelf regions. Alternatively the decreasing trend in ice duration may be linked to the heat content of the shelf, and thus ice duration is an indication of warming conditions that favor *S. thompsoni* blooms.

In addition, due the relatively short life cycle and the fixed timing of the summer cruise we cannot eliminate the possibility that *Salpa thompsoni* always blooms on the shelf, just later in some years than others. For example, although the *S. thompsoni* distribution and abundance in 93Jan was very similar to the climatology and *S. thompsoni* was not found across the shelf, a few months later in April, *S. thompsoni* was found in moderate abundance throughout the northern and mid-shelf regions (Ross et al. 1996). At the higher latitudes of the PAL grid, sampling in January may be early enough in the seasonal succession of *S. thompsoni* blooms that summer data alone will

not reveal whether *S. thompsoni* will co-occur with *Euphausia superba* later in the austral fall. Questions remain about whether the occurrence of *S. thompsoni* on the shelf in the PAL grid in January is a matter of the timing of the *S. thompsoni* blooms year to year, and not the presence or absence of *S. thompsoni* on the shelf for the entire year.

Distributions of *Limacina helicina* also correlated best with the number of ice days the previous winter. Far less is known about timing in the life cycle of *L. helicina* than the other species, but with the postulated 1.5 yr life span and spawning in January, spawning success the previous summer will impact the population size the next year. Perhaps an early advance and long duration of ice shorten the time when conditions for spawning of this pteropod are adequate, and then the numbers the next summer are lower. Alternatively a long duration of ice could impact growth and survival of the pteropods during the austral spring, leading to a lower number of individuals.

One suggestion is that *Euphausia superba* are more often associated with areas of the grid that had the most persistent ice cover during the preceding winter. But given the low correlation coefficient overall, the association is likely not driving overall population abundance, but instead influences within-year distribution. The lack of strong correlations with seasonal sea-ice parameters, given what we know about the linkage of *E. superba* to sea-ice during multiple times in their life cycle deserves some discussion. The current analysis correlates the distribution and abundance of the entire population, young and old, with sea-ice dynamics the previous year. Given the long life span and multiple points during that life span that sea-ice dynamics impacts the population dynamics of *E. superba* (Quetin and Ross, 2001; Quetin and Ross, 2003), it is not likely that a single year will encompass a large part of the variability in the spatial distribution and abundance of *E. superba*. A better comparison might be the abundance

and distribution of young-of-the-year found in January with the seasonal sea-ice dynamics of the previous year.

For the *Euphausia crystallorophias*, the seaward extent of the distribution was well correlated with the timing of retreat. The implication is that in those years when the surface waters on the inner shelf and inside Marguerite Bay were more apt to be fresher and colder due to the recent influence of melting pack ice, *E. crystallorophias* were more abundant. The melting sea-ice, and consequent colder fresher water in the surface layers, may have a direct effect on the distribution of the ice krill.

Conclusion

Clear patterns in the temporal/spatial distribution of the 5 numerically dominant macrozooplanktonic species in the Palmer LTER study region have been documented, with patterns for the shorter-lived and more oceanic species (*Salpa thompsoni*, *Limacina helicina*) more similar to each other than to the longer-lived euphausiid species (*Euphausia superba, Thysanöessa macrura, E. crystallorophias*). Anomaly patterns and trends for all 5 species reflected both strong interannual variability and a potential shift in 1998 that coincided with a rapid change from El Nino to La Nina conditions, and increasing heat content of shelf waters. Linkages to seasonal sea-ice parameters were also more apparent with species that either are predominantly oceanic or are associated with the presence of summer sea-ice. With this long-term analysis of the temporal/spatial variability in 5 of the macro- and mesozooplanktonic species west of the Antarctic Peninsula, we now have the basis for investigating the physical and biological variables that are likely to be integral to the mechanisms and processes driving variability in ecosystem structure.

Acknowledgements

We would like to gratefully acknowledge two research associates from the 1990s, T. Newberger and J. Jones, and all the graduate students and volunteers who were critical for the collection of the data. Without the ship-handling skills of the captains, mates and crews of the MV *Polar Duke* and ARSV *Laurence M. Gould*, and the logistical and on-board help of Antarctic Support Associates and Raytheon Polar Services personnel, the samples would never have made it to the deck for the volunteers to identify and count. Our discussions with our colleagues with the LTER have been invaluable, from tutorials on PCA analysis to discussions of various results. The long-term data analysis has been enjoyable and rewarding primarily due to our colleagues. This material is based upon work supported by the National Science Foundation, Office of Polar Programs, under Award Nos. OPP-9011927 and OPP-9632763, and OPP-0217282, The Regents of the University of California, the University of California at Santa Barbara, and the Marine Science Institute, UCSB. This is Palmer LTER contribution No. xxx.

REFERENCES

Aitchison, J., 1955. On the distribution of a positive random variable having a discrete probability mass at the origin. American Statistical Association Journal 50, 901-908.

Aitchison, J., Brown, J.A.C., 1969. The Lognormal Distribution. Cambridge University Press, Cambridge.

Atkinson, A., Siegel, V., Pakhomov, E. and Rothery, P., 2004. Long-term decline in krill stock and increase in salps within the Southern Ocean. Nature **432**, 100-103.

Brinton, E., Antezana, T., 1984. Structures of swarming and dispersed populations of krill (*Euphausia superba*) in Scotia Sea and South Shetland waters during January-March 1981, determined by bongo nets. Journal of Crustacean Biology **4**, Special No. 1, 45-66.

Domack, E., Leventer, A., Burnett, A., Bindschadler, R., Convey, P., Kirby, M., 2003. *Antarctic Peninsula Climate Variability: Historical and Paleoenvironmental Perspectives*. *Antarctic Research Series*, Vol. 79, Amer. Geophy. Union, 272 pp.

Ducklow, H.W., Baker, K., Martinson, D.G., Quetin, L.B., Ross, R.M., Smith, R.C., Stammerjohn, S.E.,Vernet, M., Fraser, W., 2007. Marine pelagic ecosystems: the West Antarctic Peninsula. Philosophical Transactions of the Royal Society B, 362, 67-94.

Foxton, P., 1966. The distribution and life-history of *Salpa thompsoni* Foxton with observations on a related species, *Salpa gerlachei* Foxton. Discovery Report 32, 1-116.

Gilbert, R.D., 1987. Statistical Methods for Environmental Pollution Monitoring. Van Nostrand Reinhold Company, New York, 320 pp.

Grachev, D.G., 1991. Frontal zone influences on the distribution of different zooplankton groups in the central part of the Indian sector of the Southern

Ocean. In: M.S. Samolova and S.O. Shumkova (Editors), Ecoloogy of Commercial Marine Hydrobionts. TINRO Press, Vladivostok, pp. 19-21 (in Russian).

Harbison, G.R., McAlister, V.L., Gilmer, R.W., 1986. The response of the salp, *Pegea confoederata*, to high levels of particulate material: starvation in the midst of plenty. Limnology Oceanography 31, 371-382.Hofmann, E.E., Huntley, M.E., 1991. GLOBEC: Southern Ocean Program GLOBEC Workshop on Southern Ocean Marine Animal Populations and Climate Change. Joint Oceanographic Institutions Incorporated.

Hofmann, E. E., Wiebe, P. H., Costa, D. P. and Torres, J. J., 2004. An overview of the Southern Ocean Global Ocean Ecosystems Dynamics program. Deep Sea Research Part II **51**, 1921-1924.

Hopkins, T. L., 1985. The zooplankton community of Croker Passage, Antarctic Peninsula. Polar Biology **4**, 161-170.

Hosie, G. W., Schultz, M. B., Kitchener, J. A., Cochran, T. G., and Richards, K., 2000. Macrozooplankton community structure off East Antarctica (80-150°E) during the austral summer of 1995/1996. Deep-Sea Research II 47, 2437-2464.

Kaplan, A., Cane, M.A., Kushnir, Y., Clement, A.C., Blumenthal, M.B., Rajagopalan, B., 1998. Analyses of global sea surface temperature 1856-1991. Journal of Geophysical Research 103, 18567-18589.

Kawaguchi, S., Ichii, T., Naganobu, M., 1999. Green krill, the indicator of micro- and nano-size phytoplankton availability to krill. Polar Biology 22, 133-136.Kawaguchi, S., Ichii, T., Naganobu, M., de la Mare, W.K., 1998. Do krill and salps compete? Contrary evidence from the krill fisheries. CCAMLR Science 5, 205-216.

Kawaguchi, S., Siegel, V., Litvinov, F., Loeb, V. and Watkins, J., 2004. Salp distribution and size composition in the Atlantic sector of the Southern Ocean. Deep Sea Research Part II **51**, 1369-1381.

Lalli, C.M., Gilmer, R.W., 1989. Pelagic Snails - The Biology of Holoplanktonic Gastropod Mollusks. Stanford University Press, Stanford, 259 pp.

Lancraft, T. M., Reisenbichler, K.R., Robison, B. H., Hopkins, T. L., and Torres, J. J., 2004. A krill-dominated micronekton and macrozooplankton community in Croker Passage, Antarctica with an estimate of fish predation. Deep-Sea Research II 51, 2247-2260.

Lipsky, J.D., 2005. AMLR 2004/2005 Field Season Report - Objectives, accomplishments, and tentative conclusions. NOAA-TM-NMFS-SWFSC-385, NMFS Southwest Fisheries Science Center, La Jolla.

Loeb, V., Siegel, V., 1993. AMLR program: krill and macrozooplankton in the Elephant Island area, January-March 1993. Antarctic Journal of the United States 28, 185-188.

Loeb, V., Siegel, V., 1994. AMLR program: krill stock structure and macrozooplankton abundance near Elephant Island, January-March 1994. Antarctic Journal of the United States 29, 000-000.Loeb, V., Siegel, V., Holm-Hansen, O., Hewitt, R., Fraser, W., Trivelpiece, W., Trivelpiece, S., 1997. Effects of sea-ice extent and krill or salp dominance on the Antarctic food web. Nature 387, 897-900.

Macintosh, N. S., 1936. Distribution of the macroplankton in the Atlantic sector of the Antarctic. Discovery Report **9**, 65-160.

Martinson, D.G., Stammerjohn, S.E., Iannuzzi, R.A., Smith, R.C., 2006-s. Palmer, Antarctica, Long-Term Ecological Research Program, first twelve years: Physical oceanography, spatio-temporal variability. Deep-Sea Research II 00, 00-00.

Massom, R.A., Stammerjohn, S.E., Smith, R.C., Pook, M.J., Iannuzzi, R.A., Adams, N., Martinson, D.G., Vernet, M., Fraser, W.R., Quetin, L.B., Ross, R.M., Massom, Y., Krouse, H.R., 2006. Extreme anomalous atmospheric circulation in the West Antarctic Peninsula region in austral spring and summer 2001/02, and its profound impact on sea-ice and biota. Journal of Climate 19, 3544-3571.

Nicol, S., Pauly, T., NBindoff, N.L., Wright, S., Thlele, D., Hosie, G.W., Strutton, P.G., Woehler, E., 2000. Ocean circulation off east Antarctica affects ecosysstem structure and sea-ice extent. Nature 406, 504-507.

Pakhomov, E.A., Froneman, P.W., Perissinotto, R., 2002. Salp/krill interactions in the Southern Ocean: spatial segregation and implications for the carbon flux. Deep-Sea Research II 49, 1881-1907.

Pennington, M., 1983. Efficient estimators of abundance, for fish and plankton surveys. Biometrics 39, 281-286.

Perissinotto, R., Pakhomov, E.A., 1998. Contribution of salps to carbon flux of marginal ice zone of the Lazarev Sea, Southern Ocean. Marine Biology 131, 25-32.

Priddle, J., Croxall, J. P., Everson, I., Heywood, R. B., Murphy, E. J., Prince, P. A., and Sear, C. B., 1988. Large-scale fluctuations in distribution and abundance of krill – A discussion of possible causes. In: Sahrhage, D. (Ed.), Antarctic Ocean and Resources Variability. Springer-Verlag, pp. 169-182.

Quetin, L.B., Ross, R.M., Frazer, T.K., and Haberman, K.L., 1996. Factors affecting distribution and abundance of zooplankton, with an emphasis on Antarctic krill, *Euphausia superba*.

In: Ross, R. M, Hofmann, E. E. & Quetin, L. B. (Eds.), Foundations for Ecological Research West of the Antarctic Peninsula. Antarctic Research Series, Vol **70**, pp. 357-371.

Quetin, L.B., Ross, R.M., 2001. Environmental variability and its impact on the reproductive cycle of Antarctic krill. American Zoologist 41, 74-89.

Quetin, L.B., Ross, R.M., 2003. Episodic recruitment in Antarctic krill, *Euphausia superba*, in the Palmer LTER study region. Marine Ecology Progress Series 259, 185-200.

Ross, R.M., Quetin, L.B., 2000. Reproduction in Euphausiacea. In: Everson, I. (Ed.), Krill: Biology, Ecology and Fisheries. Blackwell Science, Cambridge, pp. 150-181.

Ross, R.M., Quetin, L.B., Lascara, C.M., 1996. Distribution of Antarctic krill and dominant zooplankton west of the Antarctic Peninsula. In: Ross, R.M., Hofmann, E.E., Quetin, L.B. (Eds.), Foundations for Ecological Research west of the Antarctic Peninsula. American Geophysical Union, pp. 199-217.

Ross, R.M., Quetin, L.B., Haberman, K.L., 1998. Interannual and seasonal variability in short-term grazing impact of *Euphausia superba* in nearshore and offshore waters west of the Antarctic Peninsula. Journal of Marine Systems 17, 261-273.

Schnack-Schiel, S. B. and Mujica, A., 1994. The zooplankton of the Antarctic Peninsula region. In *Southern Ocean Ecology: the BIOMASS Perspective*. (ed. S. Z. El-Sayed), pp. 79-92. Cambridge, UK: Cambridge University Press.

Siegel, V., 2005. Distribution and population dynamics of *Euphausia superba*: summary of recent findings. Polar Biology 29, 1-22.

Siegel, V., Bergström, B., Mühlenhardt-Siegel, U. and Thomasson, M., 2002. Demography of krill in the Elephant Island area during summer 2001 and its significance for stock recruitment. Antarctic Science **14**, 162-170.Siegel, V., and Harm, U., 1996. The

composition, abundance, biomass and diversity of the epipelagic zooplankton communities of the southern Bellingshausen Sea (Antarctic) with special reference to krill and salps. Arch Fish Mar Res 44, 115-139.

Siegel, V., Loeb, V., 1995. Recruitment of Antarctic krill (*Euphausia superba*) and possible causes for its variability. Marine Ecology Progress Series 123, 45-56.

Siegel, V. and Piatkowski, U., 1990. Variability in the macrozooplankton community off the Antarctic Peninsula. Polar Biology **10**, 373-386.

Smith, S. L. and Schnack-Schiel, S. B., 2000. Polar zooplankton. In: Smith, W.O. (Ed.), Polar Oceanography Part B Chemistry, Biology, and Geology. Academic Press, Inc.527-598.

Stammerjohn, S.E., Martinson, D.G., Smith, R.C., Iannuzzi, R.A., 2006-s. Spatial and temporal (1992-2004) variability of sea-ice in the Palmer LTER region compared to larger and longer scale perspectives. Deep-Sea Research II 00, 00-00.

Treguer, P., Jacques, G., 1992. Dynamics of nutrients and phytoplankton, and fluxes of carbon,nitrogen and silicon in the Antarctic Ocean. Polar Biology 12, 149-162.

Vaughan, D.G., Marshall, G.J., Connolley, W.M., Parkinson, C., Mulvaney, R., Hodgson, D.A., King, J.C., Pudsey, C.J., Turner, J., 2003. Recent rapid regional climate warming on the Antarctic Peninsula. *Climatic Change,* **60**, 243-274.Vernet, M., Martinson, D.G., Iannuzzi, R.A., Stammerjohn, S.E., Kozlowski, W., Sines, K., Smith, R.C., 2006-s. Control of primary production by sea-ice dynamics in the western Antarctic Peninsula. Deep-Sea Research II 00, 00-00.

Voronina, N. M., 1998. Comparative abundance and distribution of major filter-feeders in the Antarctic pelagic zone. Journal of Marine Systems **17**, 375-390.

Ward, P., Grant, S., Brandon, M., Siegel, V., Sushin, V., Loeb, V., and Griffiths, H., 2004. Mesozooplankton community structure in the Scotia Sea during the CCAMLR 2000 survey: January-February 2000. Deep-Sea Research II **51**, 1351-1367.

Waters, K.J., Smith, R.C., 1992. Palmer LTER: A sampling grid for the Palmer LTER program. Antarctic Journal of the United States 27, 236-239.

Table 1. Palmer LTER cruise, sampling dates, transect lines surveyed, and number of stations occupied.

Cruise	Sampling Dates	Transect Lines	No. Stations
93Jan	8 Jan-6 Feb	200, 300, 400, 500, 600	43
94Jan	11 Jan-6 Feb	300, 400, 500, 600	56
95Jan	7 Jan-6 Feb	200, 300, 400, 500, 600	59
96Jan	8 Jan-9 Feb	200, 300, 400, 500, 600	59
97Jan	12 Jan-12 Feb	200, 300, 400, 500, 600	62
98Jan	29 Jan-13 Feb	200, 300, 400, 500, 600	50
99Jan	9 Jan-11 Feb	200, 300, 400, 500, 600	69
00Jan	9 Jan-24 Jan	200, 300, 400, 500, 600	42
01Jan	10 Jan-24 Jan	200, 300, 400, 500, 600	46
02Jan	8 Jan-26 Jan	200, 300, 400, 500, 600	48
03Jan	6 Jan-1 Feb	200, 300, 400, 500, 600	51
04Jan	8 Jan-31 Jan	200, 300, 400, 500, 600	53

Table 2. Seasonal sea-ice parameters utilized (see Stammerjohn et al., this volume for details of analysis)

Seasonal sea-ice parameter	Definition
Ice advance	Julian day when sea-ice first appears in a cell at a concentration of 15%, and persists for at least 5 d
Ice retreat	Julian day when sea-ice disappears from a cell at a concentration of 15%, and stays away for at least 5 d
Ice days	Total number of ice days of 15% concentration present between advance and retreat (counted)
Persistence	Percent of time cell covered by ice at a concentration of 15%, or ice days/(ice retreat – ice advance)

Table 3. Species to species correlation coefficients, r for climatologies. Arranged from species with most to least association with offshore, deep water.

Species	*S thomp*	*Lim hel*	*Thy mac*	*E superba*	*E crystall*
S thomp	1	+0.10	+0.34	-0.15	-0.17
Lim hel		1	+0.43	-0.27	-0.29
Thy mac			1	-0.12	-0.20
E superba				1	+0.54
E crystall					1

Table 4. Zooplankton species to ice parameter correlation coefficients, r for climatologies. Arranged from species with most to least association with offshore, deep water. Heterogeneous correlation maps shown for 'r's in bold.

Ice parameter	*S thomp*	*Lim hel*	*Thy mac*	*E superba*	*E crystall*
Ice advance	+0.70	+0.73	+0.55	+0.15	-0.68
Ice retreat	-0.65	-0.78	-0.44	+0.06	**+0.86**
Ice days	**-0.74**	**-0.78**	-0.54	-0.02	+0.84
Persistence	-0.63	-0.13	-0.41	**+0.07**	+0.45

Table 5. Modes dominated by variance in a specific year.

Species/Mode	Mode 1	Mode 2	Mode 3
Salpa thompsoni	Interannual variability in grid-wide abundance	Regional shifts in 2 'salp' years (97, 99)	
Limacina helicina	PC minimum in 1998; EOF share 1998 anomalies	PC less variable 1998-2004; EOF share features 97 anom	EOF share features of 2003 anom
Euphausia superba	6-yr cycle, with peaks in cycle in PC max in 96/97 and 02/03	Partially reflect 1998 and 2004 anomalies	PC changed pattern with 1998 year
Thysanöessa macrura	1998	Represent anom pattern 98-04	1995
Euphausia crystallorophias	Interannual variability (>+10 in 2001; < -10 in 2000 and 2004)	Reflect var in small region west of Adelaide I	1993

FIGURE LEGENDS

Figure 1. *Salpa thompsoni*: climatology of abundance (ind $1000m^{-3}$) shown on PAL grid with LTER gridlines on the y-axis and LTER stations on the x-axis. Islands are in grey. Color scale to right of panel. Isobaths are 450 m, 750 m, and1500 m. Heavy black line divides the coastal and shelf regions, dotted black line the slope and shelf regions. AnI, Anvers Island; AdI, Adelaide Island; MB, Marguerite Bay.

Figure 2. *Salpa thompsoni*: Each panel, labeled with the year above, shows the anomalies of abundance for one year of the 12-yr time series. Color scale horizontal between panels. LTER gridlines are on the y-axis and LTER stations on the x-axis. Islands are in grey. Isobaths are 450 m, 750 m, and1500 m.

Figure 3. Cumulative percentage of variance in abundance of the five species of zooplankton explained by increasing number of modes.

Figure 4. *Salpa thompsoni*: Results of PCA analysis. PC (panel above, year on x-axis) and EOF (panel below, color scale immediately to right): (A) mode 1, (B) mode 2. PAL LTER gridline and stations, and isobaths as in Fig. 1.

Figure 5. *Salpa thompsoni*: Linear trend in abundance, i.e. slope of a least squares linear regression of anomaly of abundance versus year for each grid cell shown on PAL grid with LTER gridlines on the y-axis and stations on the x-axis. Islands are in grey. Heavy black line divides the coastal and shelf regions, dotted black line the slope and shelf regions.

Figure 6. *Limacina helicina*: climatology of abundance (ind $1000m^{-3}$) shown on PAL grid with LTER gridlines on the y-axis and LTER stations on the x-axis. Islands are in grey. Color scale to right of panel. Isobaths are 450 m, 750 m, and1500 m. Heavy

black line divides the coastal and shelf regions, dotted black line the slope and shelf regions. AnI, Anvers Island; AdI, Adelaide Island; MB, Marguerite Bay.

Figure 7. *Limacina helicina*: Each panel, labeled with the year above, shows the anomalies of abundance for one year of the 12-yr time series. Color scale horizontal between panels. LTER gridlines are on the y-axis and LTER stations on the x-axis. Islands are in grey. Isobaths are 450 m, 750 m, and1500 m.

Figure 8. *Limacina helicina:* Results of PCA analysis. PC (panel above, year on x-axis) and EOF (panel below, color scale immediately to right): (A) mode 1, (B) mode 2. PAL LTER gridline and stations, and isobaths as in Fig. 1.

Figure 9. *Limacina helicina*: Linear trend in abundance, i.e. slope of a least squares linear regression of anomaly of abundance versus year for each grid cell shown on PAL grid with LTER gridlines on the y-axis and stations on the x-axis. Islands are in grey. Heavy black line divides the coastal and shelf regions, dotted black line the slope and shelf regions.

Figure 10. *Euphausia superba*: climatology of abundance (ind $1000m^{-3}$) shown on PAL grid with LTER gridlines on the y-axis and LTER stations on the x-axis. Islands are in grey. Color scale to right of panel. Isobaths are 450 m, 750 m, and1500 m. Heavy black line divides the coastal and shelf regions, dotted black line the slope and shelf regions. AnI, Anvers Island; AdI, Adelaide Island; MB, Marguerite Bay.

Figure 11. *Euphausia superba*: Each panel, labeled with the year above, shows the anomalies of abundance for one year of the 12-yr time series. Color scale horizontal between panels. LTER gridlines are on the y-axis and LTER stations on the x-axis. Islands are in grey. Isobaths are 450 m, 750 m, and1500 m.

Figure 12. *Euphausia superba*: Results of PCA analysis. PC (panel above, year on x-axis) and EOF (panel below, color scale immediately to right): (A) mode 1, (B) mode 2. PAL LTER gridline and stations, and isobaths as in Fig. 1.

Figure 13. *Thysanöessa macrura*: climatology of abundance (ind $1000m^{-3}$) shown on PAL grid with LTER gridlines on the y-axis and LTER stations on the x-axis. Islands are in grey. Color scale to right of panel. Isobaths are 450 m, 750 m, and1500 m. Heavy black line divides the coastal and shelf regions, dotted black line the slope and shelf regions. AnI, Anvers Island; AdI, Adelaide Island; MB, Marguerite Bay.

Figure 14. *Thysanöessa macrura*: Each panel, labeled with the year above, shows the anomalies of abundance for one year of the 12-yr time series. Color scale horizontal between panels. LTER gridlines are on the y-axis and LTER stations on the x-axis. Islands are in grey. Isobaths are 450 m, 750 m, and1500 m.

Figure 15. *Thysanöessa macrura*: Results of PCA analysis. PC (panel above, year on x-axis) and EOF (panel below, color scale immediately to right): (A) mode 1, (B) mode 2. PAL LTER gridline and stations, and isobaths as in Fig. 1.

Figure 16. *Euphausia crystallorophias*: climatology of abundance (ind $1000m^{-3}$) shown on PAL grid with LTER gridlines on the y-axis and LTER stations on the x-axis. Islands are in grey. Color scale to right of panel. Isobaths are 450 m, 750 m, and1500 m. Heavy black line divides the coastal and shelf regions, dotted black line the slope and shelf regions. AnI, Anvers Island; AdI, Adelaide Island; MB, Marguerite Bay.

Figure 17. *Euphausia crystallorophias*: Each panel, labeled with the year above, shows the anomalies of abundance for one year of the 12-yr time series. Color scale horizontal between panels. LTER gridlines are on the y-axis and LTER stations on the x-axis. Islands are in grey. Isobaths are 450 m, 750 m, and1500 m.

Figure 18. *Euphausia crystallorophias*: Results of PCA analysis. PC (panel above, year on x-axis) and EOF (panel below, color scale immediately to right): (A) mode 1, (B) mode 2. PAL LTER gridline and stations, and isobaths as in Fig. 1.

Figure 19. Heterogeneous correlation map of log abundance of *Salpa thompsoni* and number of ice days the previous year, with 1 year lag. Interpolated correlation coefficient (r) for each grid cell shown on PAL grid with LTER gridlines on the y-axis and stations on the x-axis, color bar to right of panel. Islands are in grey. Heavy black line divides the coastal and shelf regions, dotted black line the slope and shelf regions.

Figure 20. Heterogeneous correlation map of log abundance of *Limacina helicina* and number of ice days the previous year, with 1 year lag. Interpolated correlation coefficient (r) for each grid cell shown on PAL grid with LTER gridlines on the y-axis and stations on the x-axis, color bar to right of panel. Islands are in grey. Heavy black line divides the coastal and shelf regions, dotted black line the slope and shelf regions.

Figure 21. Heterogeneous correlation map of log abundance of *Euphausia superba* and ice persistence the previous year, with 1 year lag. Interpolated correlation coefficient (r) for each grid cell shown on PAL grid with LTER gridlines on the y-axis and stations on the x-axis, color bar to right of panel. Islands are in grey. Heavy black line divides the coastal and shelf regions, dotted black line the slope and shelf regions.

Figure 22. Heterogeneous correlation map of log abundance of *Euphausia crystallorophias* and julian day of ice retreat the previous year, with 1 year lag. Interpolated correlation coefficient (r) for each grid cell shown on PAL grid with LTER gridlines on the y-axis and stations on the x-axis, color bar to right of panel. Islands are in

grey. Heavy black line divides the coastal and shelf regions, dotted black line the slope and shelf regions.

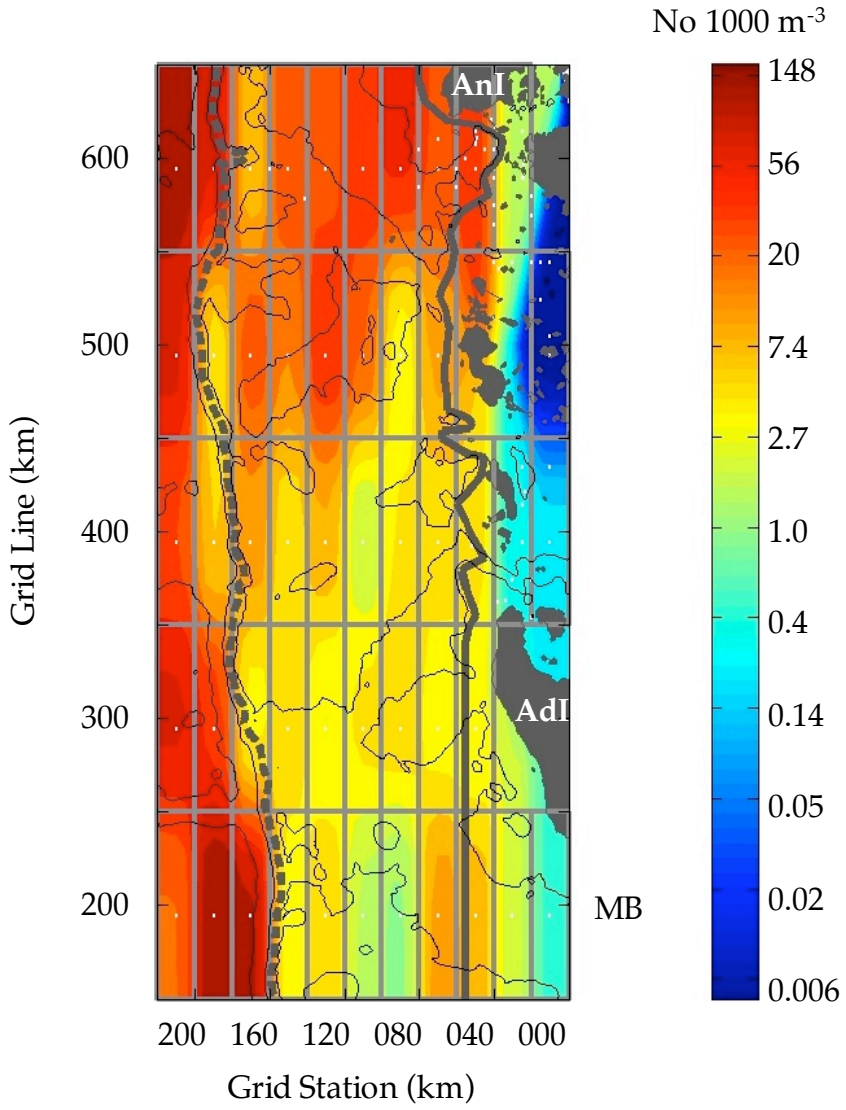
No 1000 m-3
148
56
20
7.4
2.7
1.0
0.4
0.14
0.05
0.02
0.006
AnI
AdI
MB
600
500
400
300
200
Grid Line (km)
200 160 120 080 040 000
Grid Station (km)

Fig. 1

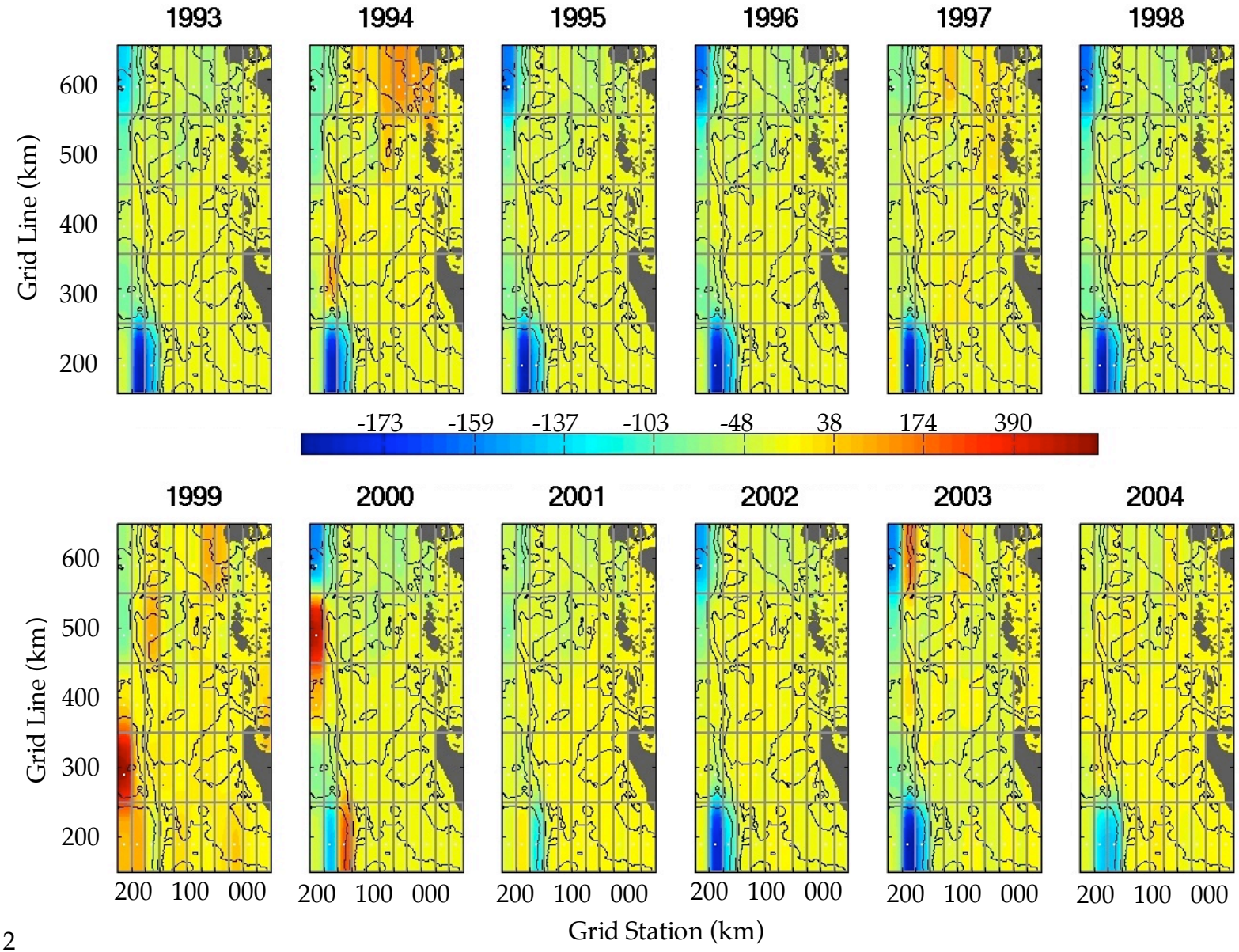
1993
1994
1995
1996
1997
1998
1999
2000
2001
2002
2003
2004
Grid Line (km)
600
500
400
300
200
-173
-159
-137
-103
-48
38
174
390
200
100
000
Grid Station (km)

Fig. 2

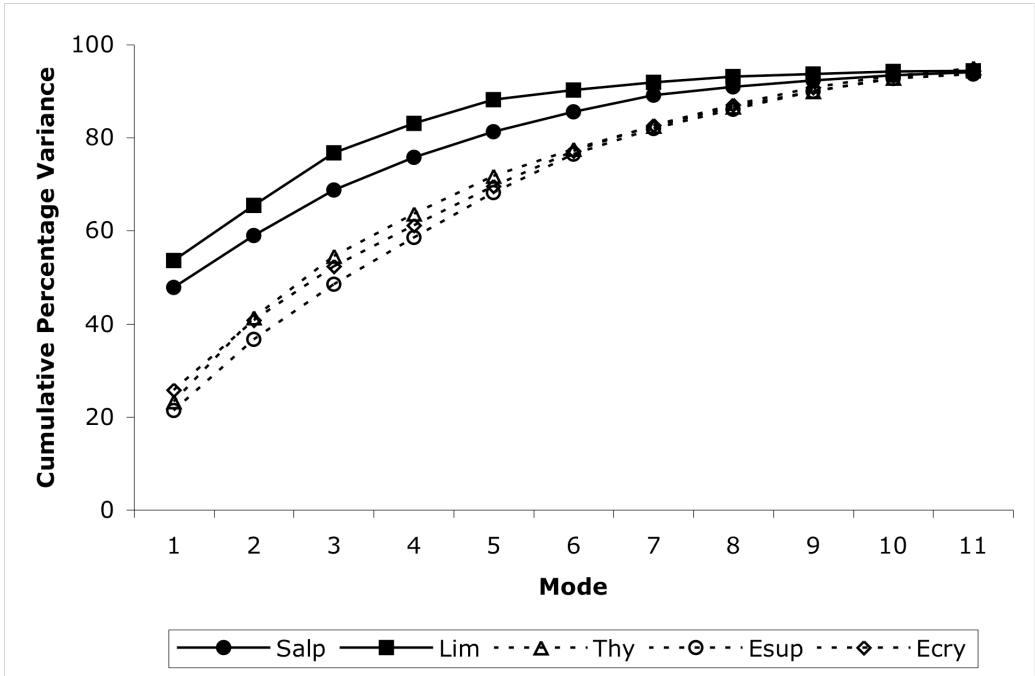
Cumulative Percentage Variance
100
80
60
40
20
0
1
2
3
4
5
6
7
8
9
10
11
Mode
Salp
Lim
Thy
Esup
Ecry

Fig. 3

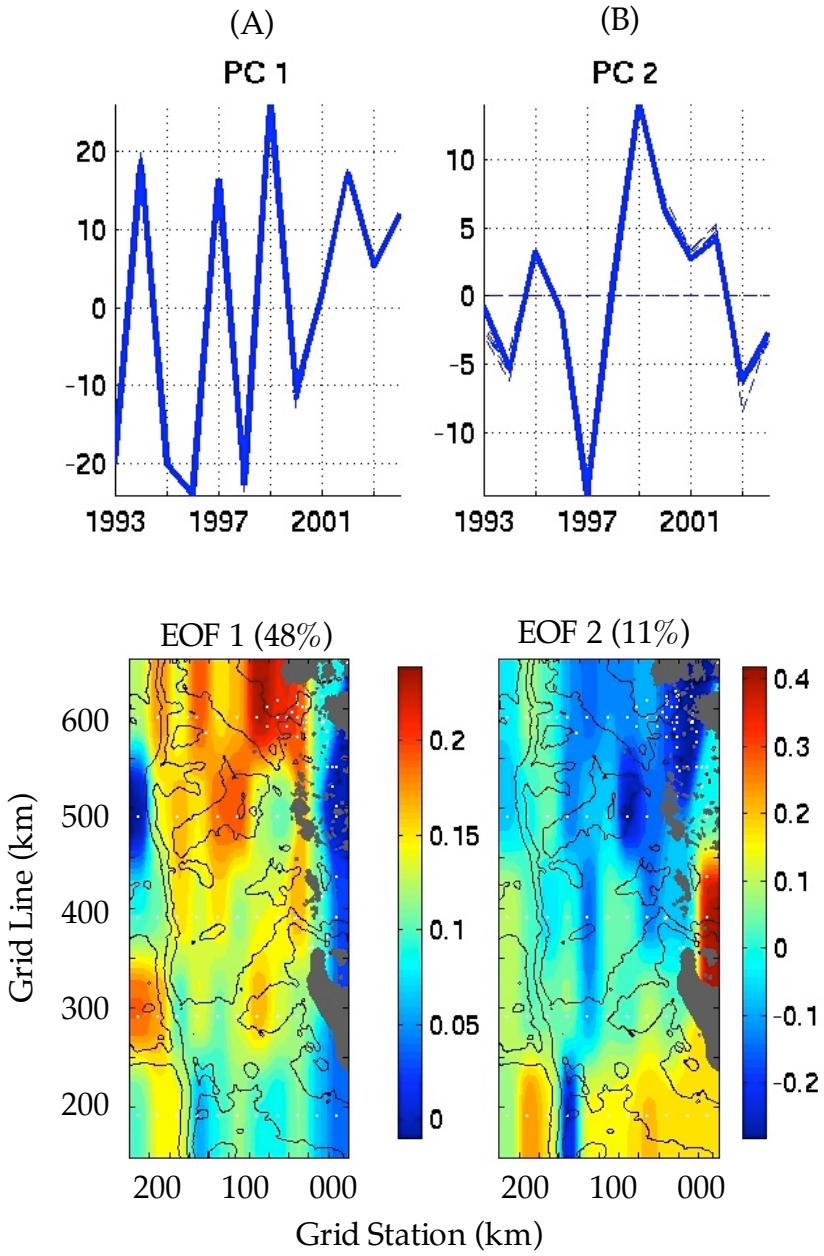
(A)
PC 1
20
10
0
-10
-20
1993
1997
2001
(B)
PC 2
10
5
0
-5
-10
1993
1997
2001
EOF 1 (48%)
EOF 2 (11%)
Grid Line (km)
600
500
400
300
200
0.2
0.15
0.1
0.05
0
0.4
0.3
0.2
0.1
0
-0.1
-0.2
200
100
000
200
100
000
Grid Station (km)

Fig. 4

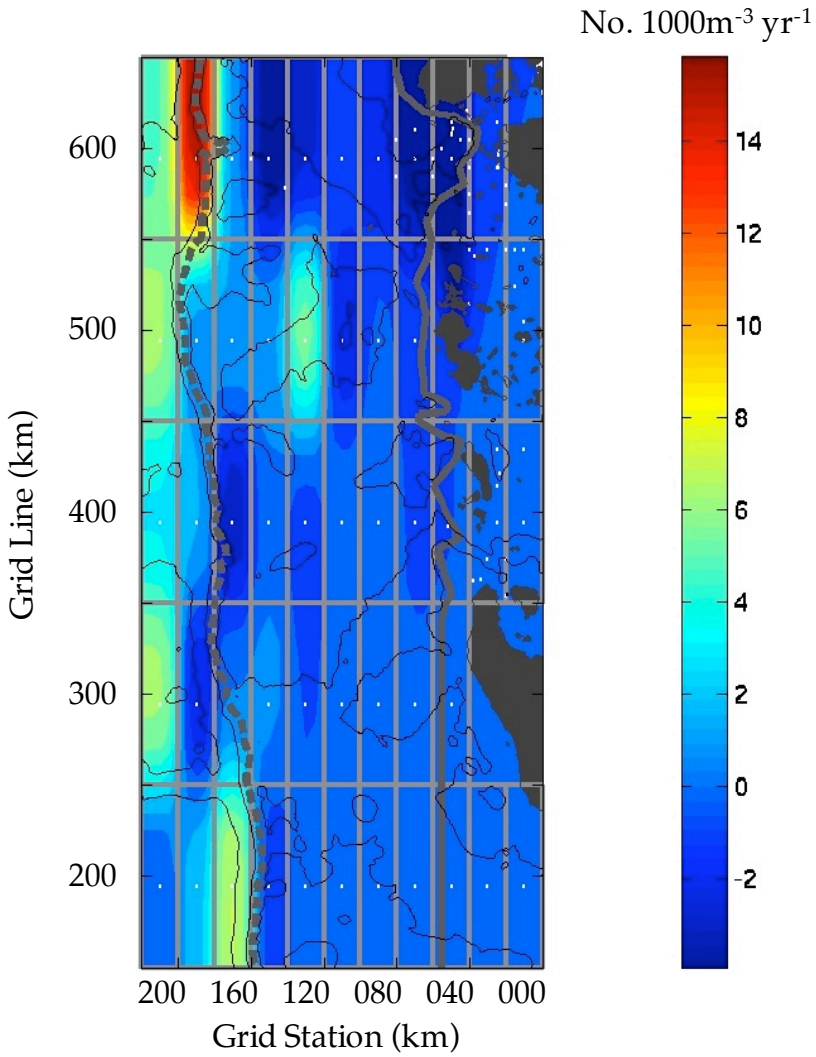
No. 1000m-3 yr-1
14
12
10
8
6
4
2
0
-2
600
500
400
300
200
Grid Line (km)
200 160 120 080 040 000
Grid Station (km)

Fig. 5

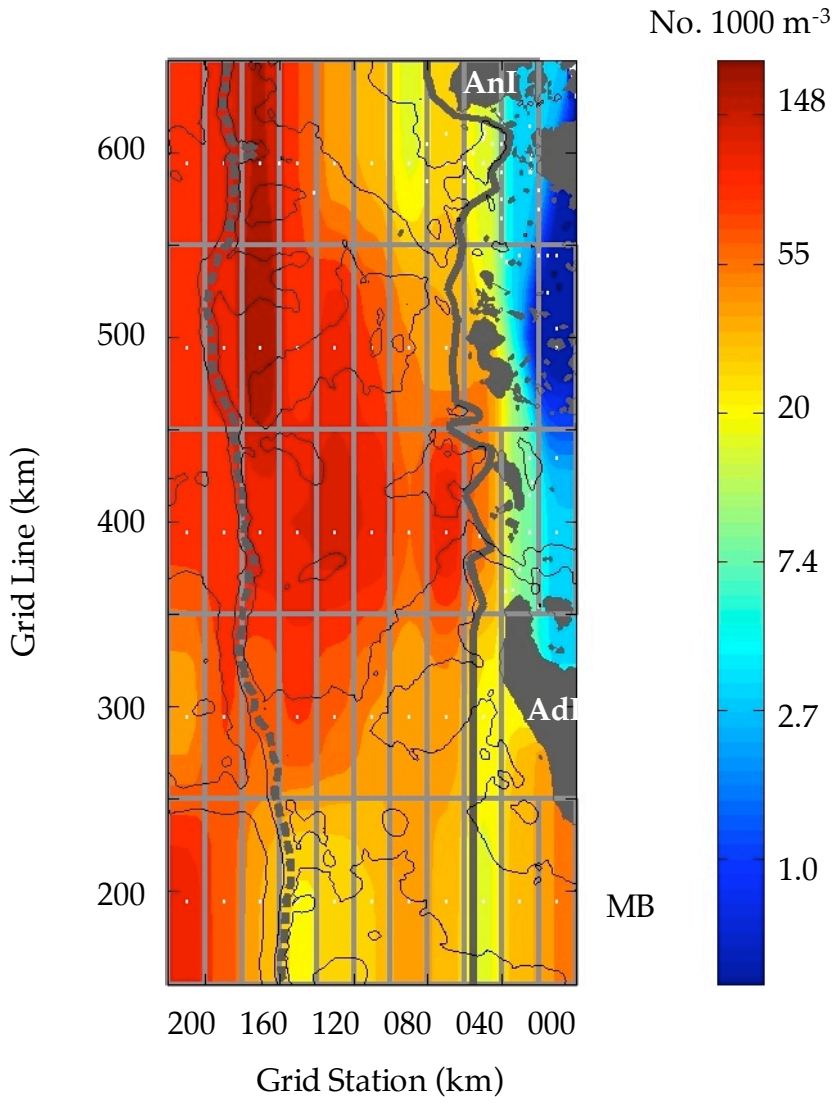
No. 1000 m-3
148
55
20
7.4
2.7
1.0
AnI
AdI
MB
600
500
400
300
200
Grid Line (km)
200 160 120 080 040 000
Grid Station (km)

Fig. 6

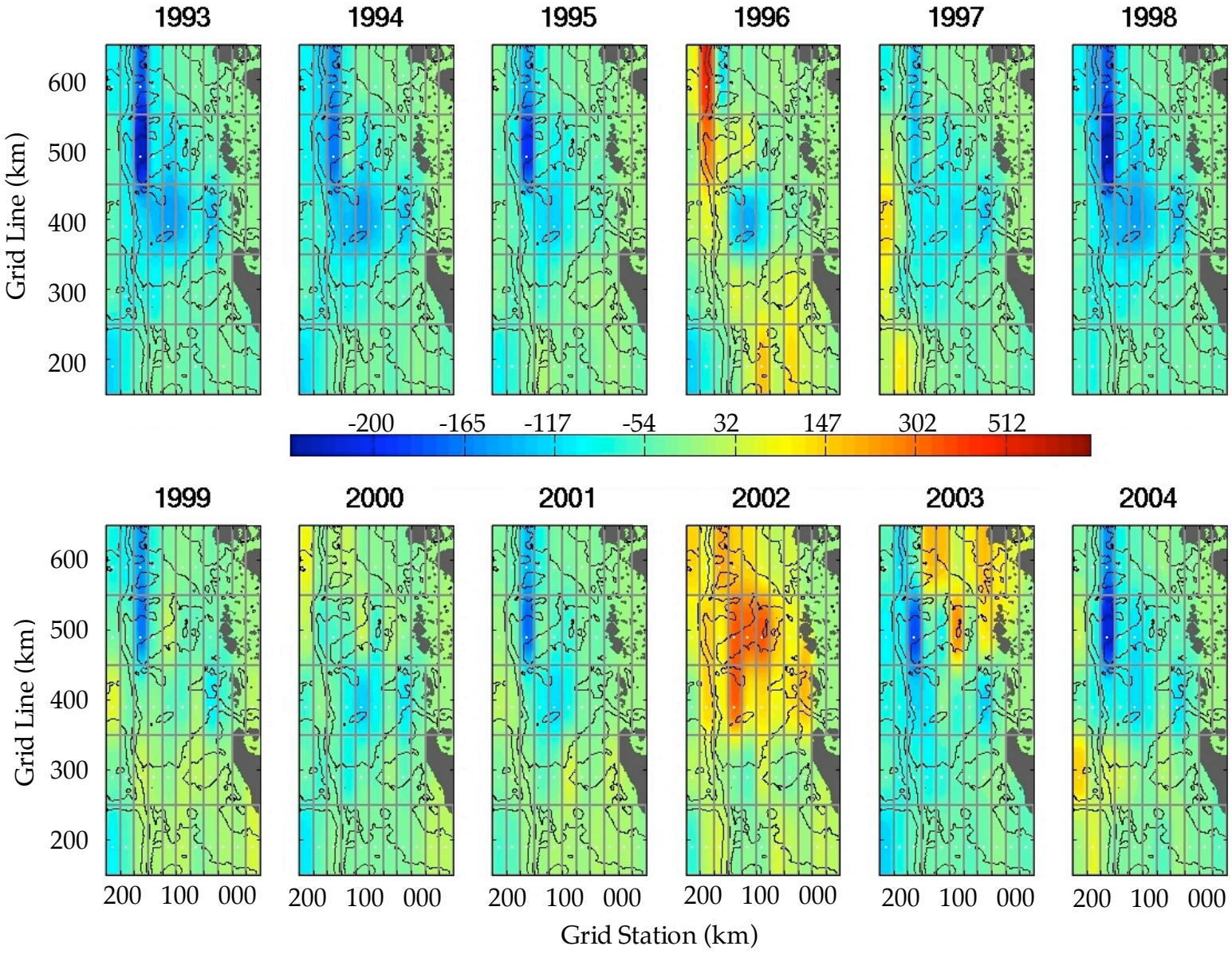
1993
1994
1995
1996
1997
1998
1999
2000
2001
2002
2003
2004
Grid Line (km)
600
500
400
300
200
-200
-165
-117
-54
32
147
302
512
200
100
000
Grid Station (km)

Fig. 7

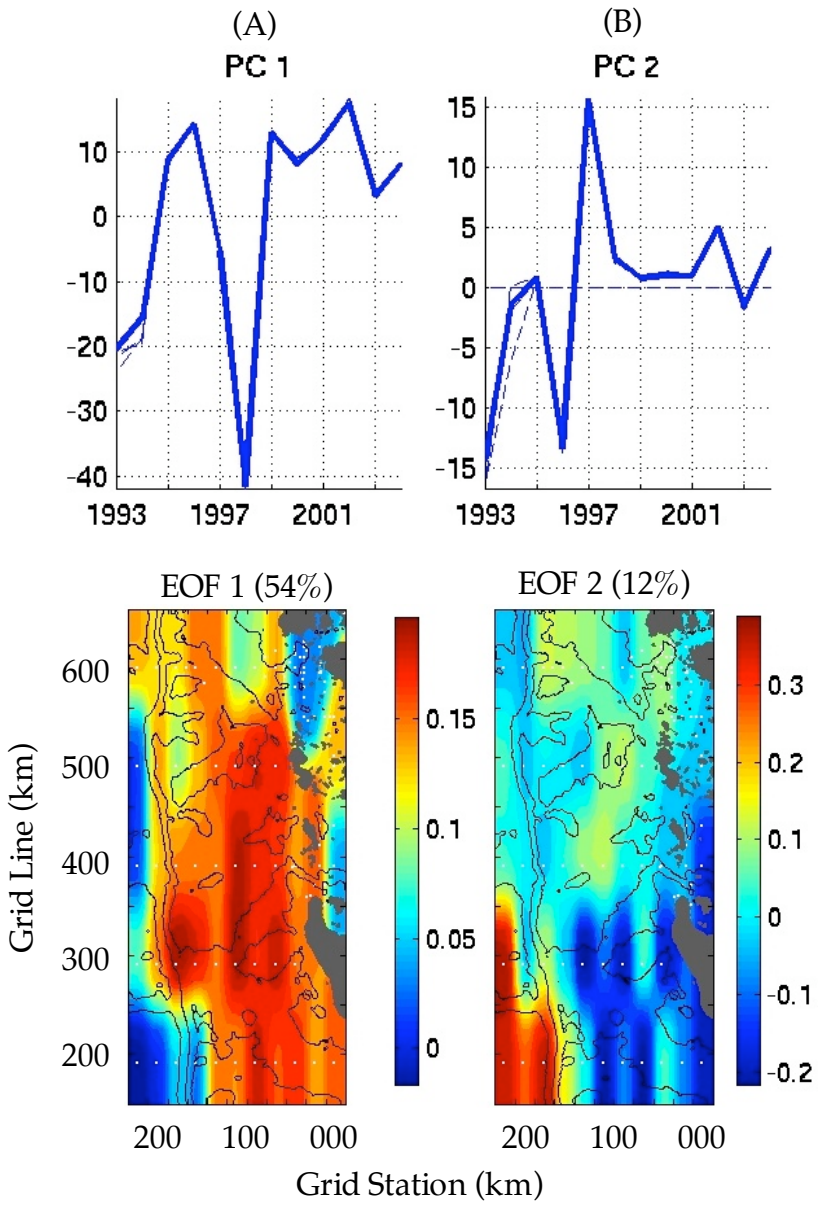
(A)
PC 1
(B)
PC 2
10
0
-10
-20
-30
-40
1993
1997
2001
15
10
5
0
-5
-10
-15
1993
1997
2001
EOF 1 (54%)
EOF 2 (12%)
Grid Line (km)
600
500
400
300
200
0.15
0.1
0.05
0
0.3
0.2
0.1
0
-0.1
-0.2
200
100
000
200
100
000
Grid Station (km)

Fig. 8

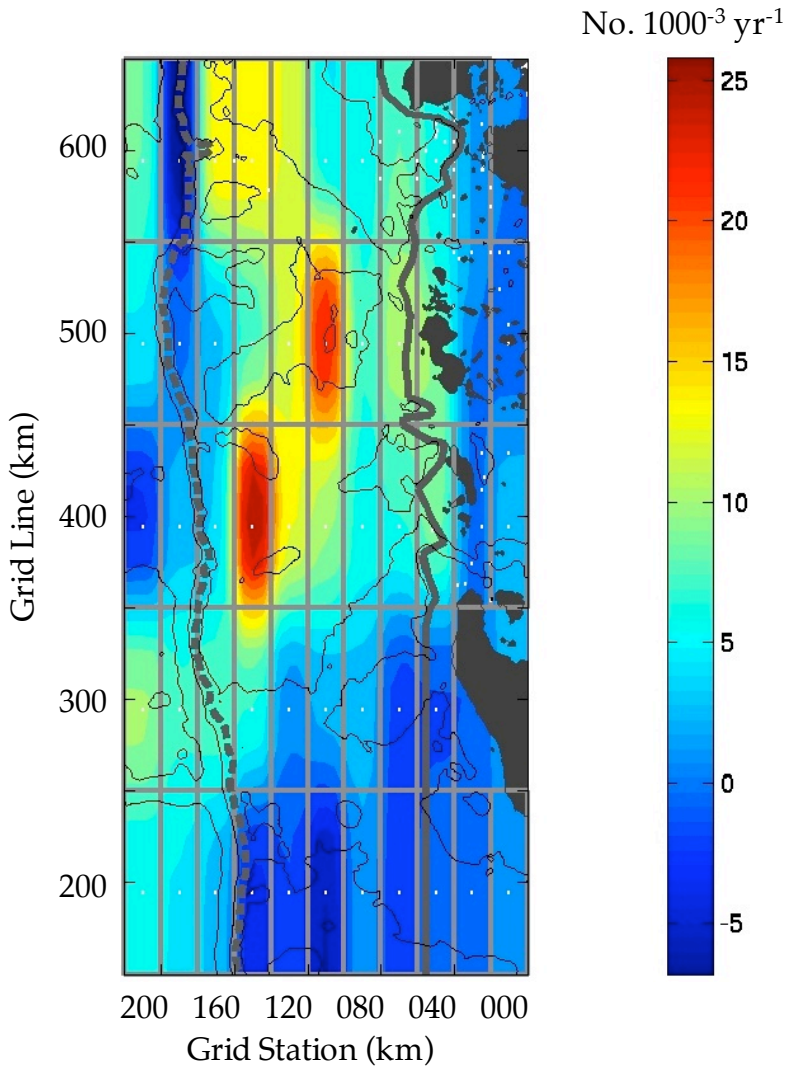
No. 1000-3 yr-1
25
20
15
10
5
0
-5
600
500
400
300
200
Grid Line (km)
200 160 120 080 040 000
Grid Station (km)

Fig. 9

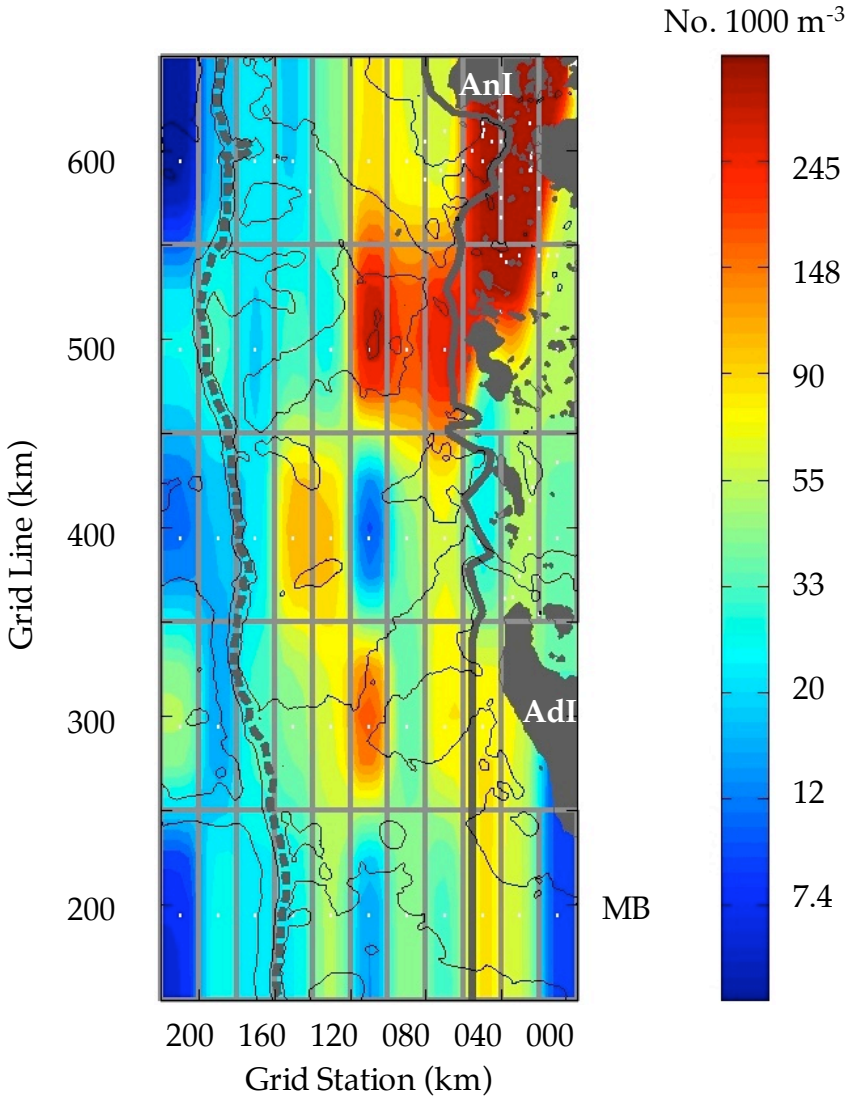
No. 1000 m-3
245
148
90
55
33
20
12
7.4
AnI
AdI
MB
600
500
400
300
200
Grid Line (km)
200 160 120 080 040 000
Grid Station (km)

Fig. 10

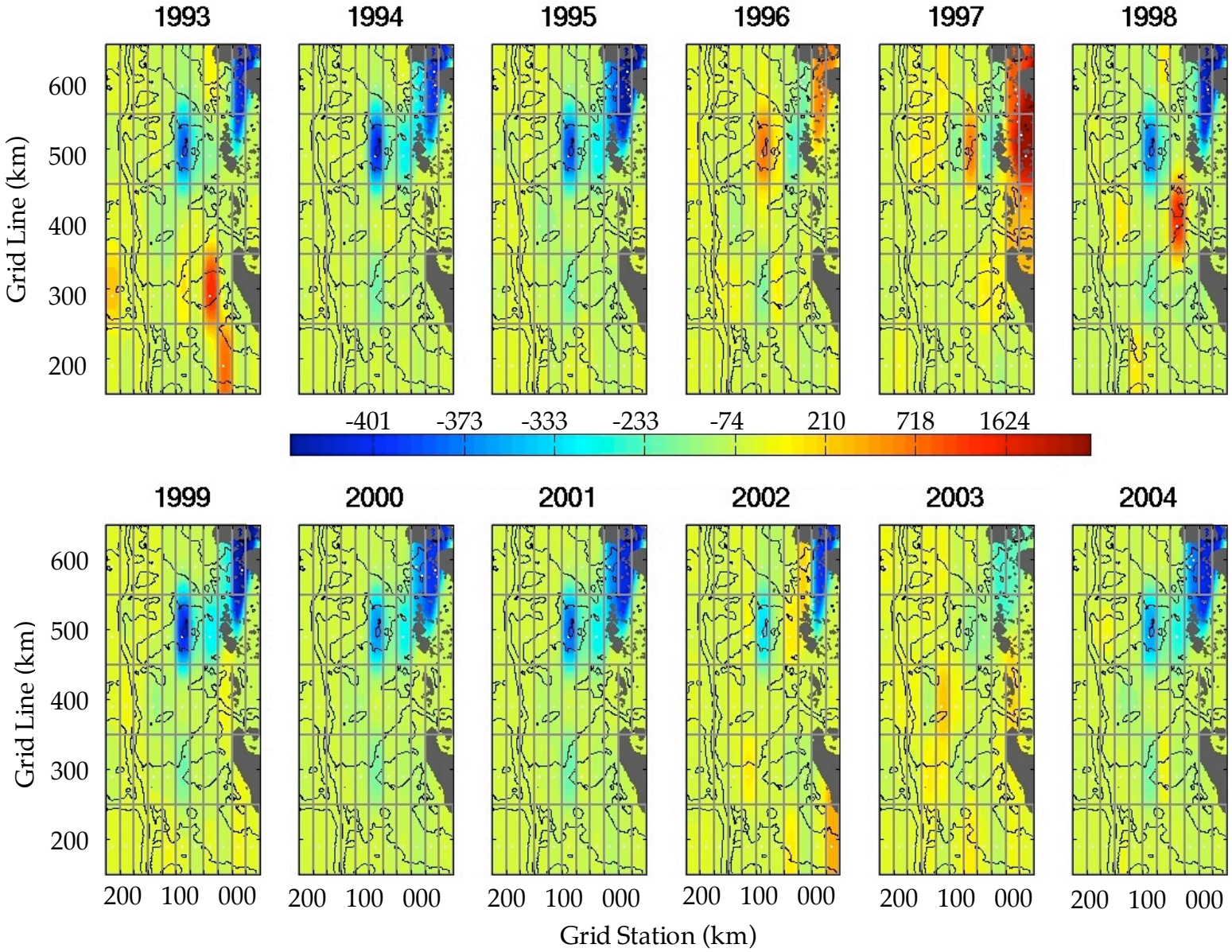
1993
1994
1995
1996
1997
1998
1999
2000
2001
2002
2003
2004
Grid Line (km)
600
500
400
300
200
-401
-373
-333
-233
-74
210
718
1624
200
100
000
Grid Station (km)

Fig. 11

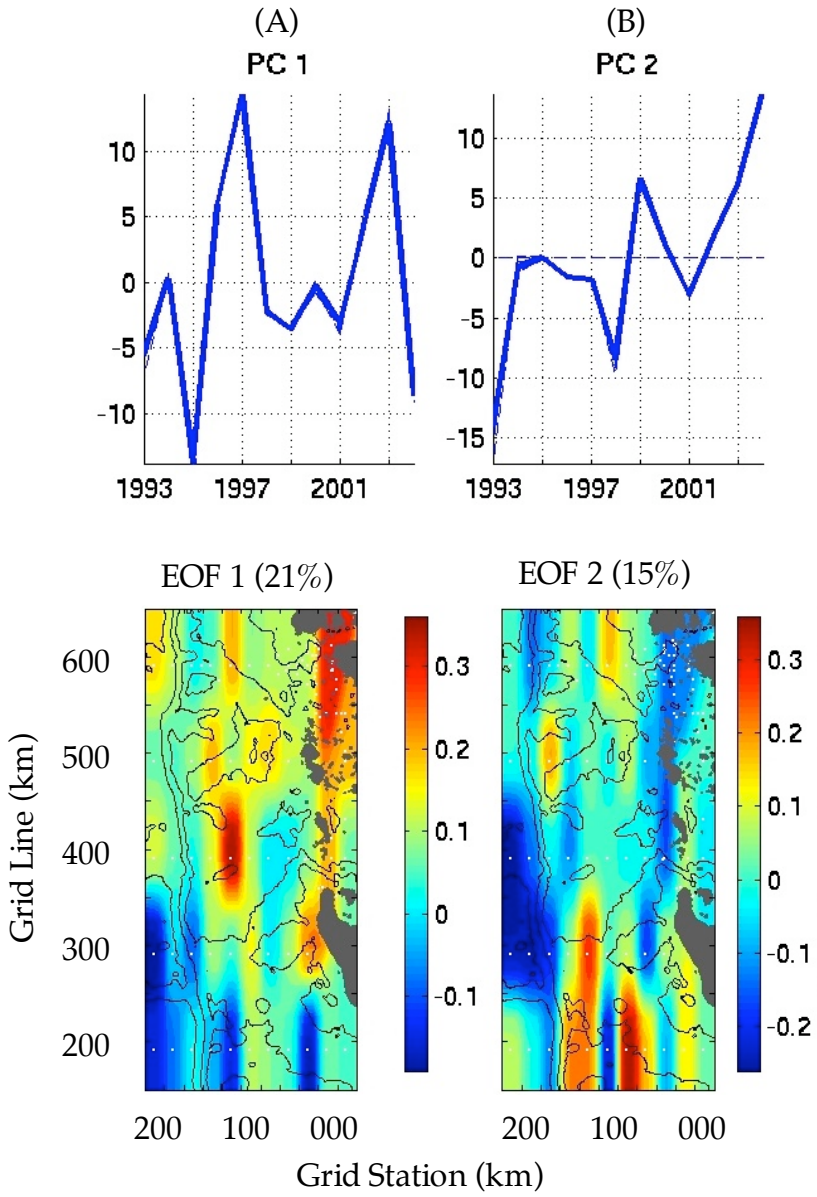
(A)
PC 1
(B)
PC 2
10
5
0
-5
-10
-15
1993
1997
2001
EOF 1 (21%)
EOF 2 (15%)
Grid Line (km)
600
500
400
300
200
0.3
0.2
0.1
0
-0.1
-0.2
200
100
000
Grid Station (km)

Fig. 12

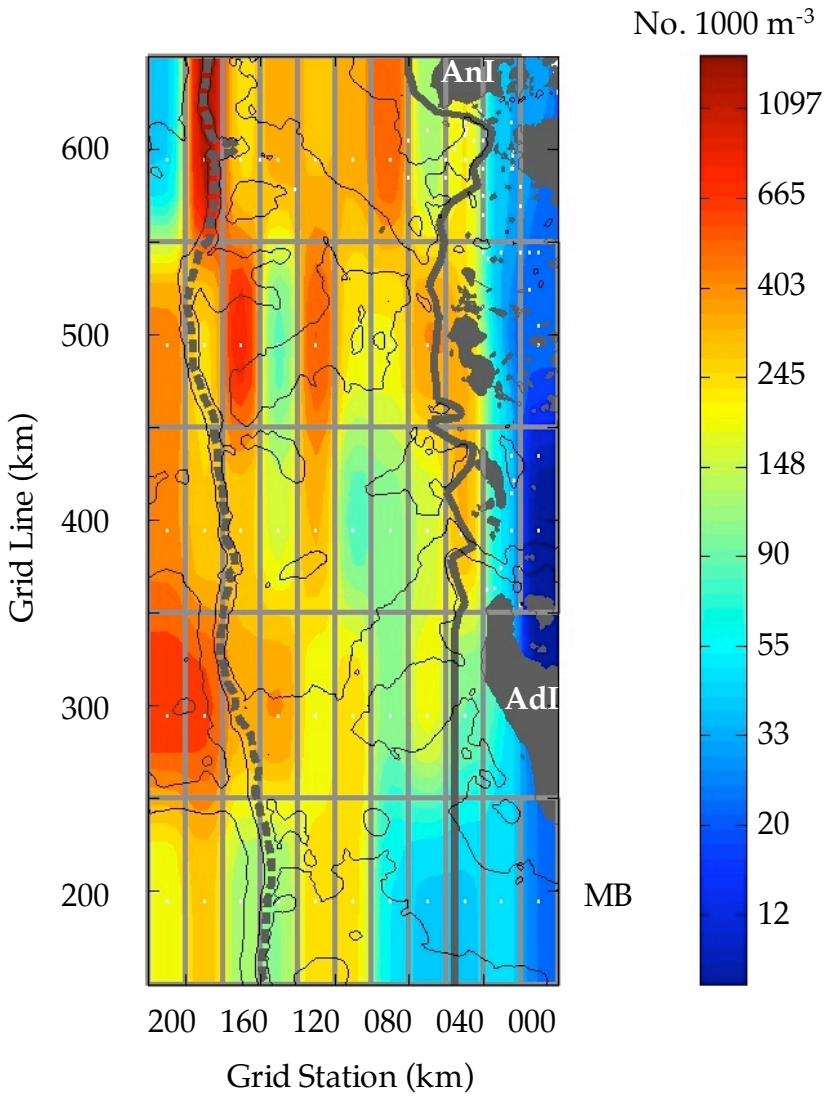
No. 1000 m-3
1097
665
403
245
148
90
55
33
20
12
AnI
AdI
MB
600
500
400
300
200
Grid Line (km)
200 160 120 080 040 000
Grid Station (km)

Fig. 13

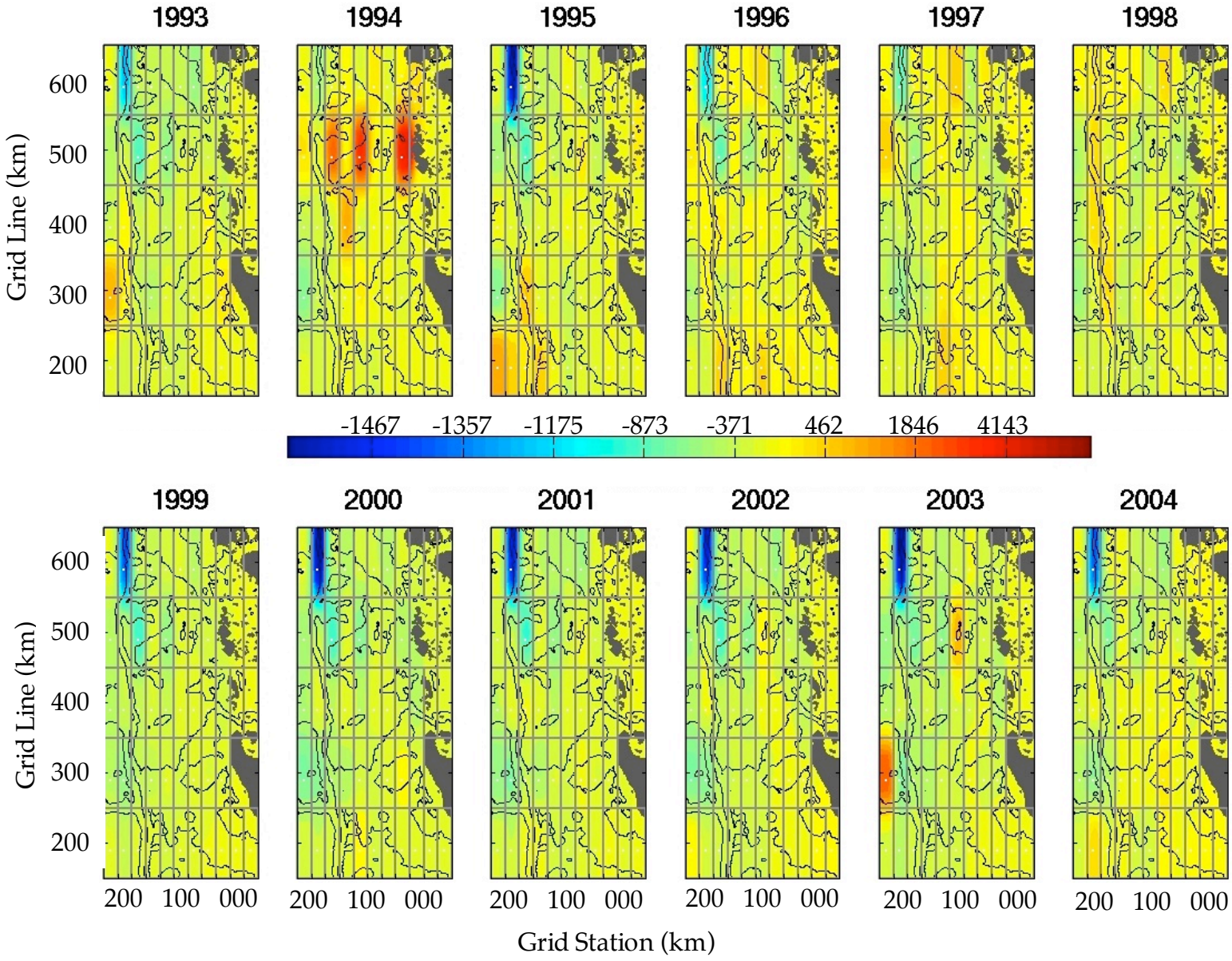
1993
1994
1995
1996
1997
1998
1999
2000
2001
2002
2003
2004
Grid Line (km)
600
500
400
300
200
-1467
-1357
-1175
-873
-371
462
1846
4143
200 100 000
Grid Station (km)

Fig. 14

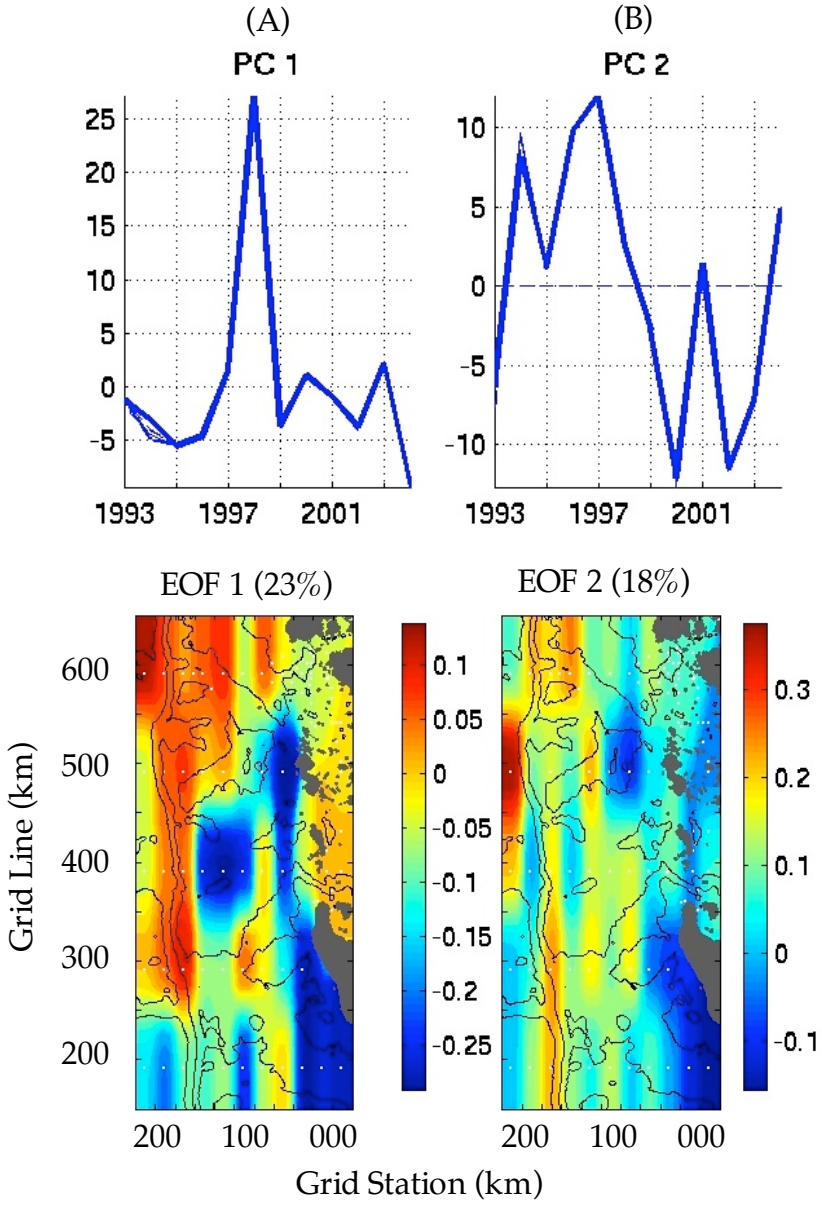
(A)
PC 1
(B)
PC 2
25
20
15
10
5
0
-5
1993
1997
2001
10
5
0
-5
-10
1993
1997
2001
EOF 1 (23%)
EOF 2 (18%)
Grid Line (km)
600
500
400
300
200
0.1
0.05
0
-0.05
-0.1
-0.15
-0.2
-0.25
0.3
0.2
0.1
0
-0.1
200
100
000
200
100
000
Grid Station (km)

Fig. 15

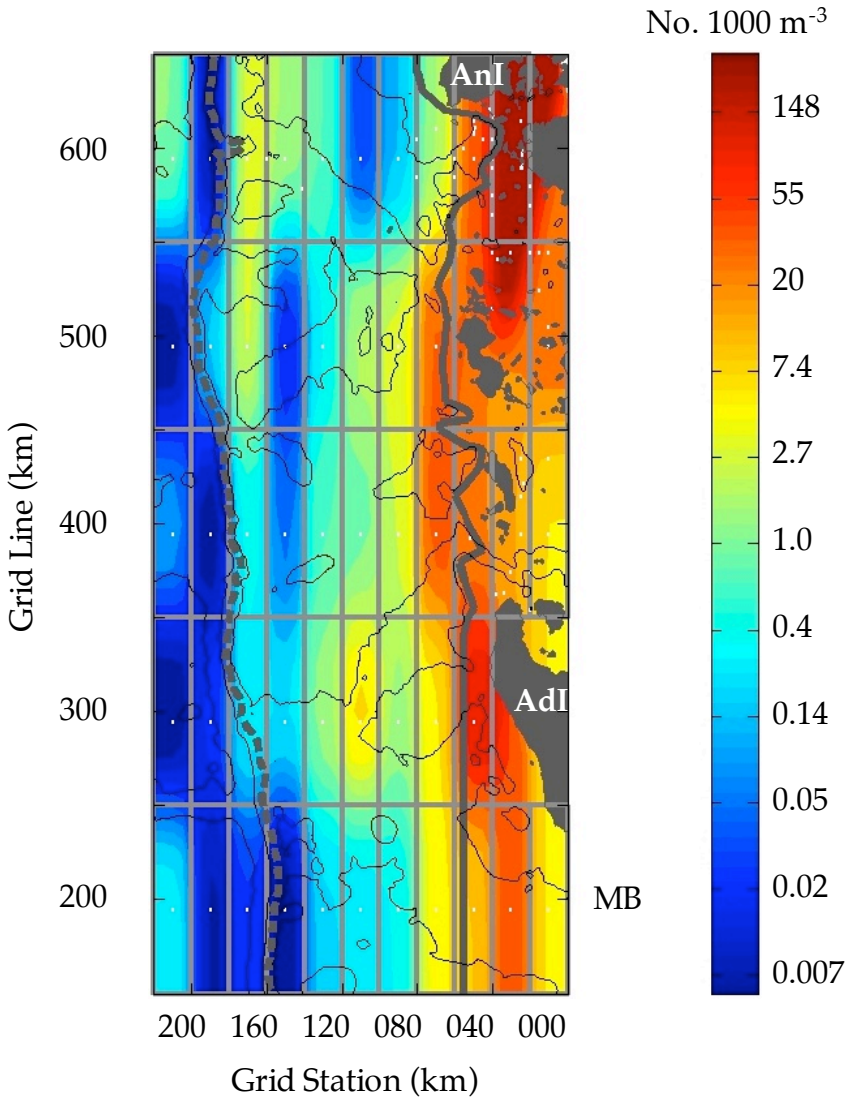
No. 1000 m-3
148
55
20
7.4
2.7
1.0
0.4
0.14
0.05
0.02
0.007
AnI
AdI
MB
600
500
400
300
200
Grid Line (km)
200 160 120 080 040 000
Grid Station (km)

Fig. 16

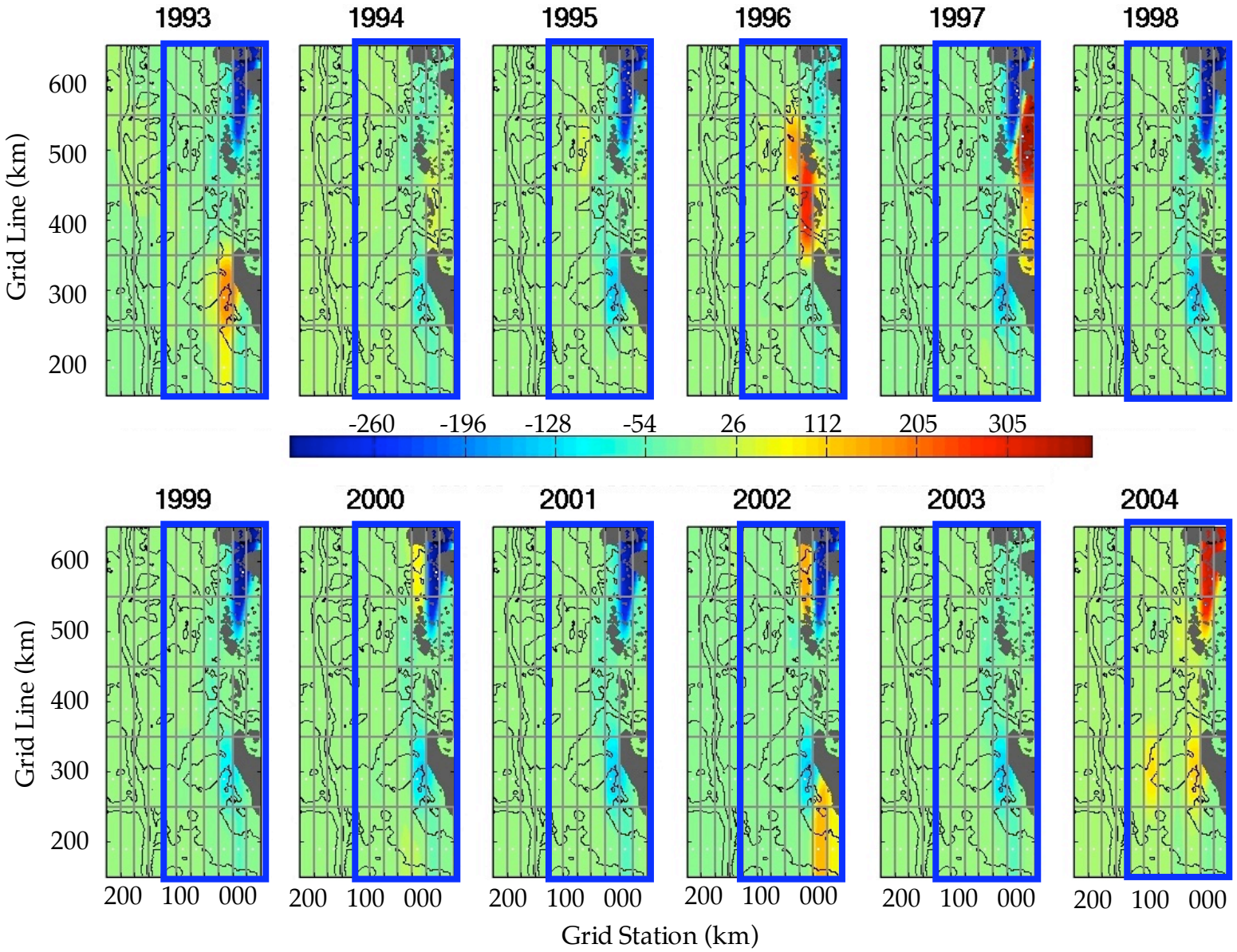
1993
1994
1995
1996
1997
1998
1999
2000
2001
2002
2003
2004
Grid Line (km)
600
500
400
300
200
-260
-196
-128
-54
26
112
205
305
200
100
000
Grid Station (km)

Fig. 17

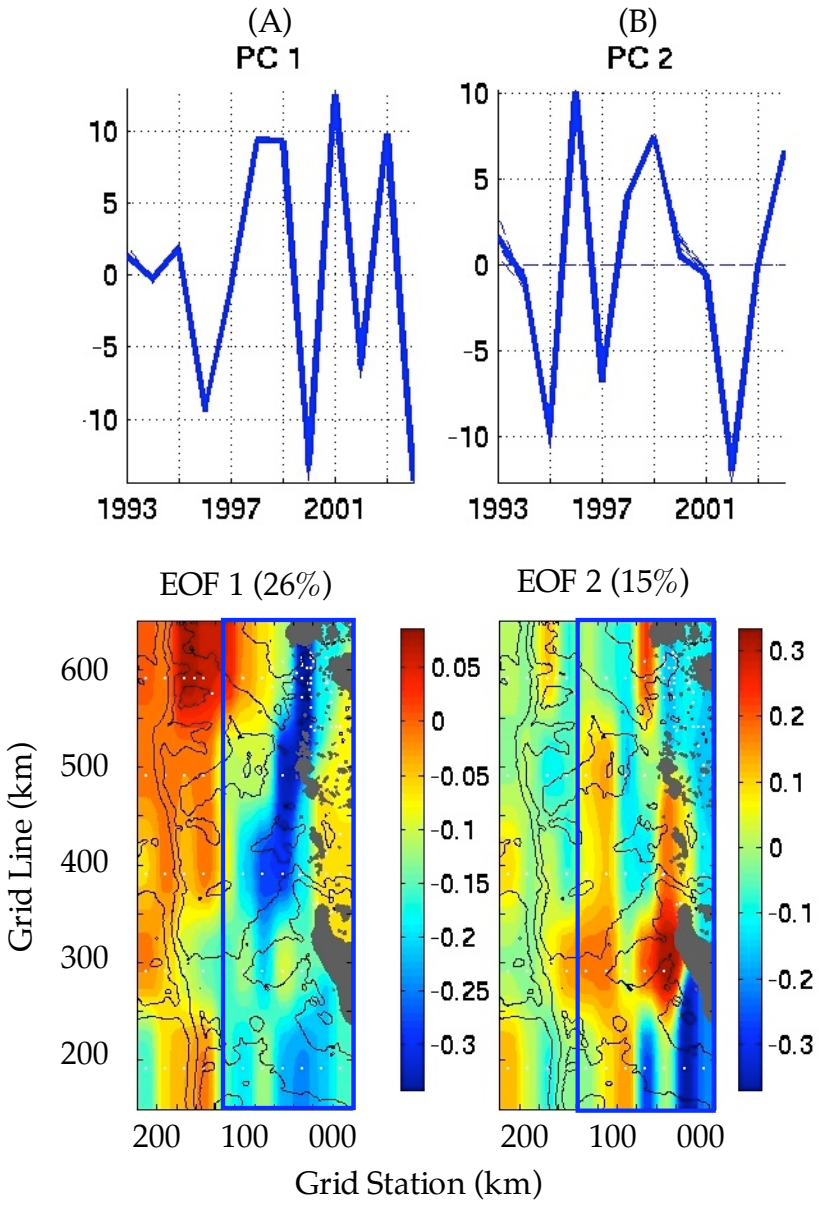
(A)
PC 1
(B)
PC 2
10
5
0
-5
-10
1993
1997
2001
EOF 1 (26%)
EOF 2 (15%)
Grid Line (km)
600
500
400
300
200
0.05
0
-0.05
-0.1
-0.15
-0.2
-0.25
-0.3
0.3
0.2
0.1
0
-0.1
-0.2
-0.3
200
100
000
Grid Station (km)

Fig. 18

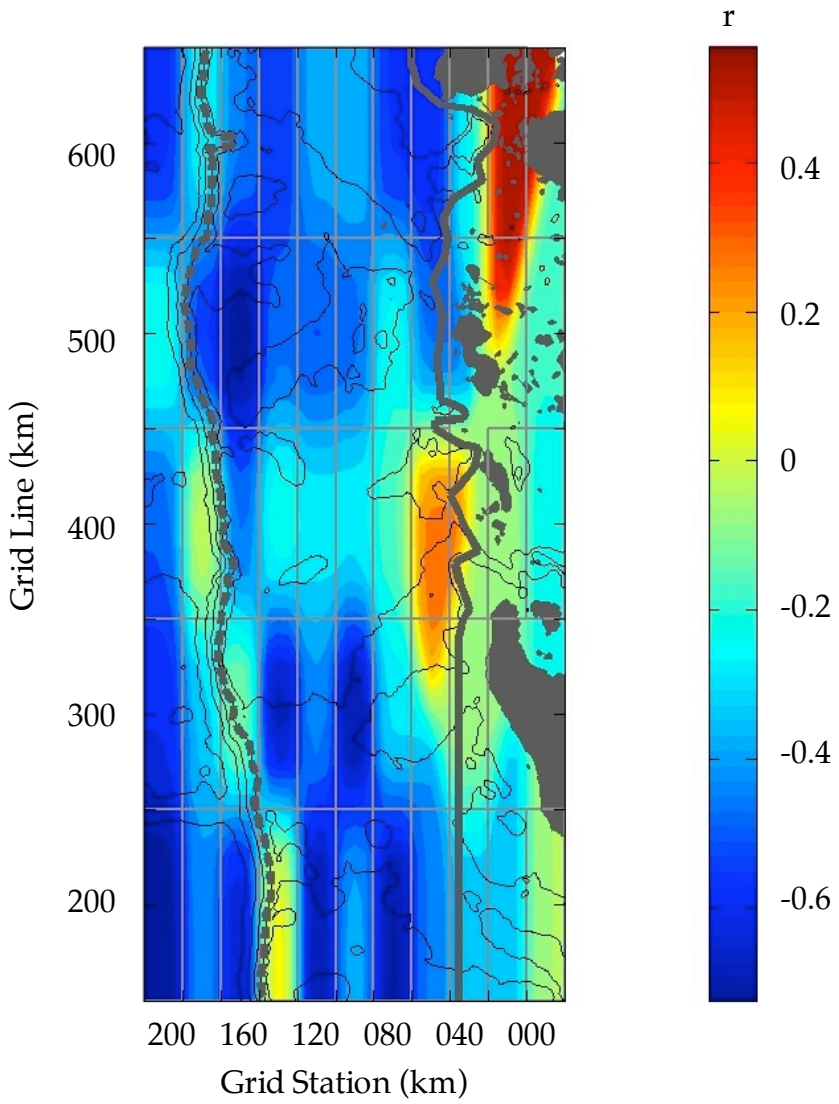
r
0.4
0.2
0
-0.2
-0.4
-0.6
600
500
400
300
200
Grid Line (km)
200 160 120 080 040 000
Grid Station (km)

Fig. 19

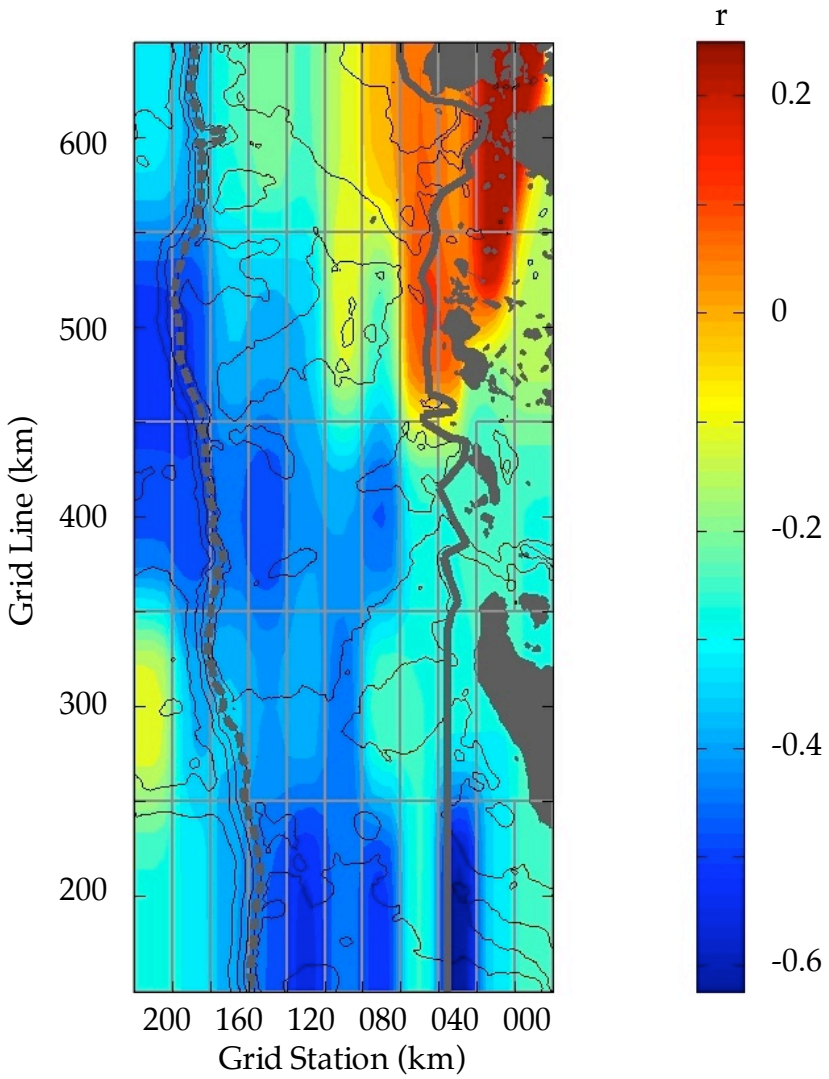
r
0.2
0
-0.2
-0.4
-0.6
600
500
400
300
200
Grid Line (km)
200 160 120 080 040 000
Grid Station (km)

Fig. 20

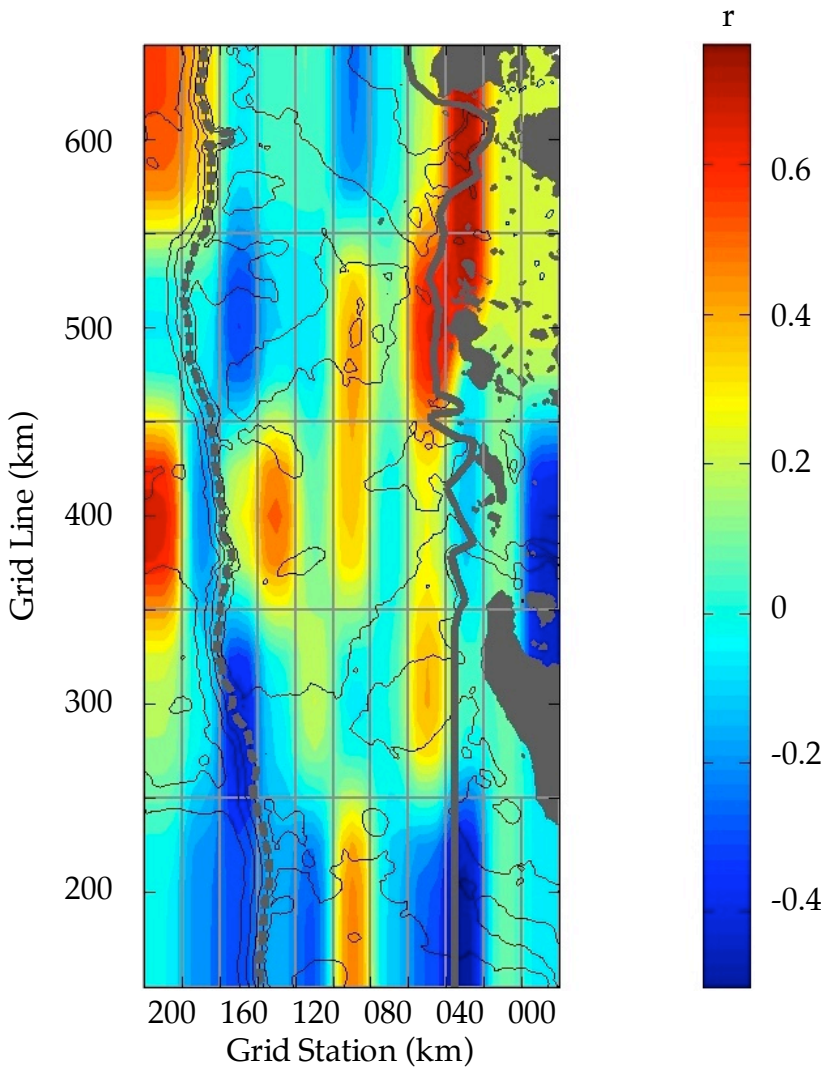
r
0.6
0.4
0.2
0
-0.2
-0.4
600
500
400
300
200
Grid Line (km)
200 160 120 080 040 000
Grid Station (km)

Fig. 21

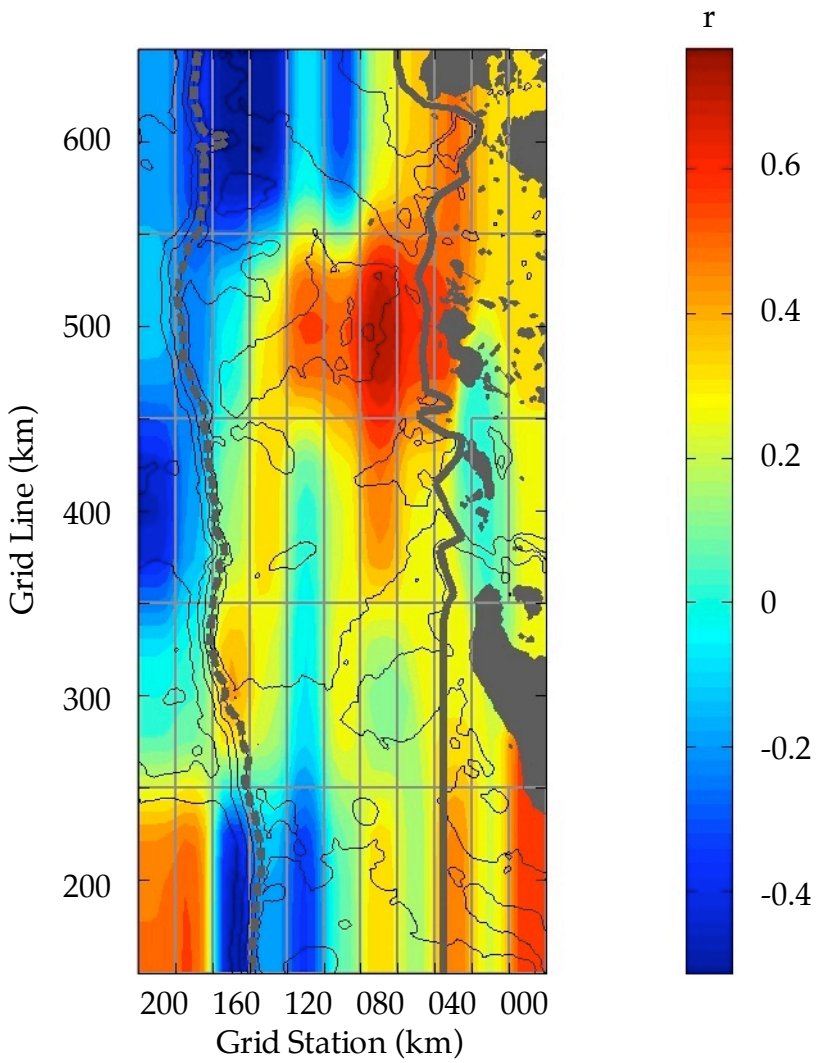
r
0.6
0.4
0.2
0
-0.2
-0.4
600
500
400
300
200
Grid Line (km)
200 160 120 080 040 000
Grid Station (km)

Fig. 22